

2m4

**NASA TECHNICAL
MEMORANDUM**

NASA TM X-62,331

NASA TM X-62,331

(NASA-TM-X-62331) A FOUR-ELEMENT END-FIRE
MICROPHONE ARRAY FOR ACOUSTIC MEASUREMENTS
IN WIND TUNNELS (NASA) 45 p HC \$4.25

N74-15913

CSCI 09A

G3/09 Unclass
28340

**A FOUR-ELEMENT END-FIRE MICROPHONE ARRAY FOR
ACOUSTIC MEASUREMENTS IN WIND TUNNELS**

Paul T. Soderman and Stephen C. Noble

Ames Research Center

and

**U. S. Army Air Mobility R&D Laboratory
Moffett Field, Calif. 94035**



January 1974

A FOUR-ELEMENT END-FIRE MICROPHONE ARRAY
FOR ACOUSTIC MEASUREMENTS IN WIND TUNNELS

Paul T. Soderman and Stephen C. Noble*

Ames Research Center

And

U. S. Army Air Mobility R&D Laboratory

Moffett Field, Calif. 94035

*Air Force Research Associate, now at Air Force Avionics Lab.,

Wright-Patterson Air Force Base, Ohio 45433

SUMMARY

A prototype four-element end-fire microphone array was designed and built for evaluation as a directional acoustic receiver for use in large wind tunnels. The microphone signals were digitized, time delayed, summed, and reconverted to analog form in such a way as to create a directional response with the main lobe along the array axis. The measured array directivity agrees with theoretical predictions confirming the circuit design of the electronic control module.

The array with 0.15 m (0.5 ft) microphone spacing rejected reverberations and background noise in the Ames 40- by 80-Foot Wind Tunnel by 5 to 12 dB for frequencies above 400 Hz.

NOTATION

c	speed of sound
d	Microphone spacing, cm (ft)
dB	decibel
f	frequency of sound
U	wind speed, m/s (f/s)
α	directivity angle relative to array axis
λ	acoustic wavelength

INTRODUCTION

Various directional acoustic receivers are being developed for measuring noise in the Ames 40- by 80-Foot Wind Tunnel. These receivers are needed to discriminate between the desired acoustic signal and the reverberant and background noise in the wind tunnel. Ideally, sound close to that which would be obtained in anechoic space could be measured by pointing a directional receiver having low sensitivity to wind across the wind tunnel at the source. This would alleviate masking of aircraft noise by a) reverberations due to a closed hardwall test section, b) background noise from the wind tunnel fans, and c) microphone wind noise.

A linear end-fire* array of microphones is one such directional receiver being evaluated. Each microphone signal is delayed and summed with the other microphone signals so that sound waves traveling down the array axis sum in phase and sound waves off axis sum out of phase, tending to cancel. For ordinary end-fire operation the signals from microphones 1, 2, 3, and 4

*An end-fire array has the main directivity lobe along the line of elements as opposed to a broadside array which has the main lobe perpendicular to the line of elements.

(fig. 1) are delayed 0 , t , $2t$, and $3t$ seconds, respectively, where $t = d/c$ is the time for sound to travel between microphones.

Microphone arrays are antennas, the general theory of which has been well developed (refs. 1-3). Microphone arrays have been used widely in underwater acoustics (refs. 4-5). Both General Electric Co. (ref. 6) and the Boeing Co.* have used broadside arrays to measure jet engine noise. Reference 6 has an excellent discussion of the various types of linear arrays which could be used specifically for acoustic measurements.

INSTRUMENTATION AND APPARATUS

The array was comprised of four omnidirectional microphones (B&K model 4133) mounted to a 2.54 cm (1 in.) diameter pipe as shown in figures 1 and 2. The microphone signals were input to the electronic control module which digitized, delayed, summed, and reconverted the signals to analog form. The data were then analyzed in third-octave bands. Delay of each channel from 0 to 10 milliseconds in 1 microsecond steps could be chosen by the operator. It was discovered that 10 microsecond steps would have been sufficient since smaller delay affected signal summation only when the microphones were spaced impracticably close together. The control module was made entirely with integrated circuit components. Design details of the control module will be published in a report on the development of an eight channel array.

TESTING AND PROCEDURE

Directivity response was measured in an anechoic chamber by rotating the array on a turntable 4 m (13 ft) from a fixed loudspeaker. Proper delay for ordinary end-fire response depends only on the time of wave propagation from one element to another, not frequency, and was chosen in such a way that sound waves traveling along the array summed in phase. The array was also operated without delay resulting in a broadside directivity response.

The array was tested in the 40- by 80-foot wind tunnel at test section speeds of 0, 18, and 28 m/s (0, 58, 92 f/s). The array was aimed at a horn driver mounted near the center of the test section 6.7 m (22 ft) away as shown in figures 2(a) and (b). The omnidirectional microphones with nose cones were pointed into the wind for low wind noise. The source was driven with octave bands of pink (random) noise. The electronic gain of the array output was removed from the data so that the array response at $\alpha = 0^\circ$ would have been equal to that of an omnidirectional microphone with both devices in anechoic space. The effect of wind speed on wave propagation time was not incorporated in the time delays used, resulting in some erroneous high frequency array data which have been omitted.

RESULTS AND DISCUSSION

Figures 3(a)-(c) show the directivity pattern of the array measured in an anechoic chamber for various values of d/λ (ratio of microphone spacing to acoustic wave length). Microphone spacing was 15 cm (0.5 ft). As expected, the array performance depended on the ratio d/λ . Figure 3(d) shows that the same directivity resulted for two different spacing (15 cm and 30 cm)

*Conversation with Jack O'Keefe, the Boeing Co.

as long as d/λ was unchanged. The measured directivity agreed fairly well with theoretical predictions based on reference 1 as shown in figures 3(b) and (f). The best directivity resulted when d/λ was in the limits of $0.35 \leq d/\lambda \leq 0.88$. Above that limit side lobes grew (high frequency) and below that limit the main lobe broadened (low frequency). Therefore, if the measured frequency doubles, the spacing should be changed (for this prototype) to maintain an optimum value of d/λ . A nonuniform spacing of 15, 30, and 46 cm (0.5, 1.0, 1.5 ft) between successive microphones resulted in the directivity pattern shown in figures 4(a)-(c). The directivity for the nonuniform spacing was no better than that resulting from 30 cm (1 ft) uniform spacing (fig. 3(d)) and has a main lobe with larger side lobes than was measured with a 15 cm (0.5 ft) spacing (fig. 3(b)).

Figures 5(a) and (b) show end-fire response compared to broadside response, the latter response resulting when signal delay was zero. The broadside was more directional than end-fire as expected (ref. 6), but the back lobe was as strong as the front lobe. Since the main lobe of a broadside array is disc shaped, sound is accepted equally well from the front, back, above, or below. This is a disadvantage in a reverberant space such as the 40- by 80-foot wind tunnel and must be compensated for by using directional microphones or a cross of two arrays which would still have a back lobe (ref. 7). An end-fire lobe, on the other hand, is shaped like a flashlight beam.

Since much aerodynamic noise is broadband and unsteady, array directivity was measured with the loudspeaker driven by a random noise generator. Figure 6 shows that with random noise filtered in octave bands, the valleys between minor lobes were eliminated. Since the microphone spacing was fixed, the difference in frequencies between the low and high ends of the octave band correspond to a doubling of d/λ . As mentioned above, a doubling of d/λ necessitates a change of microphone spacing. To achieve optimum directivity, therefore, broadband noise should be filtered in third-octave bands or narrower and spacing should be adjusted for the desired frequency so that d/λ is kept within proper limits. If the directivity of figure 6 is acceptable, octave bands can, of course, be used. The dependency of directivity on frequency, and hence d/λ , is related to the phase cancellation of off-axis sound. The on-axis sound always sums in phase regardless of frequency or frequency band.

Figures 7(a)-(h) show the results of array acoustic measurements in the 40- by 80-foot wind tunnel with and without forward speed compared to the output of an omnidirectional microphone. Both receivers had equal sensitivity in the direction of the source ($\alpha = 0^\circ$). The array was successful in rejecting a substantial amount of reverberation and background noise when aimed at a horn driver in the test section. The source was driven by octave bands of random noise, one band at a time. The source noise at 1000 Hz was partially masked by background noise due to wind tunnel operation, but the 2000 and 4000 Hz noise was greater than background levels. The data show that the array rejected 5 to 7 dB of noise in the frequency bands in which the source was operating. In most cases, the array measured the same source noise level wind on and wind off. Since previous studies (ref. 8) showed that source reverberations in the 40- by 80-foot wind tunnel at the array distance are

approximately 5 to 7 dB above the direct field, figures 7(a)-(h) indicate that the array was measuring free-field noise levels of the horn driver. However, this result was not verified since a free-field calibration of the horn driver was not made.

The noise rejection of figures 7(a)-(h) is summarized in figures 8(a)-(h) as plots of Δ dB versus frequency, where

$$\Delta\text{dB} = \text{dB array} - \text{dB omnidir. microphone (algebraic subtraction)}$$

The noise outside the frequency bands in which the source was operating was due to wind tunnel fan noise and microphone wind noise. The array rejected 5 to 12 dB of this noise over a surprisingly large range of d/λ (0.18-3.53). This result can be attributed to the fact that 1) on-axis sound sums in phase regardless of d/λ , and 2) side lobes have less effect in a reverberant space than figures 3(a)-(i) suggest since it is the response integrated over a sphere which determines rejection, not just relative amplitudes of side lobes. Rejection was especially good at frequencies above 400 Hz, but the array was too short to effect low frequencies. Longer arrays with more microphones should reject noise at lower frequencies. Also, noise rejection by an array would be better if directional microphones such as the one described in reference 9 are used instead of omnidirectional microphones.

The amount of microphone noise due to wind in these experiments was not determined. However, the relative response of an end-fire to wind-generated microphone turbulence compared to the response to sound waves can be predicted. Figure 9 shows such a response assuming microphone wind noise sums incoherently (3 dB for each doubling of the number of microphones) and sound waves add coherently (6 dB for each doubling of the number of microphones). Wake impingement from one microphone on another, however, should be avoided.

To see if the experimental results of figures 8(a)-(h) are predictable, an analysis was performed to estimate how much noise a four-element array will reject in a reverberant space.

Since antenna transmission is analogous to reception (principle of reciprocity), it can be assumed for calculation purposes that the array generates sound. The sound emitted by a source in anechoic space is equivalent in terms of amplitude and directivity to the sound received in a reverberant space. Imagine the emitted sound pressure levels integrated over a sphere surrounding a directional array (i.e., the sound power) in anechoic space compared to the sound power of an omnidirectional source adjusted to give the same pressure level as the array along the array axis ($\alpha = 0^\circ$). Obviously, the omnidirectional source would emit the greater sound power by some amount Δ dB. Due to the principle of reciprocity, it follows that this Δ dB sound power is equal to the Δ dB difference in sound pressure levels measured by an omnidirectional microphone and a directional array in a reverberant space, both adjusted to have equal sensitivity at $\alpha = 0^\circ$. Thus, the emitted sound power levels of the array and an omnidirectional source were calculated in the following manner.

The array directivity pattern for 15 cm (1/2 ft) element spacing as measured in the anechoic chamber was used to represent transmission directivity. Sound power was calculated using the following relationship (ref. 10):

$$L_w = \overline{L_{ps}} + 20 \log R + 11 \quad (1)$$

L_w = total sound power level, dB re 10^{-12} watt

R = radius of sound measurement locations on a sphere surrounding the source, meters

$\overline{L_{ps}}$ = average mean-square sound pressure level over the sphere, dB re 2×10^{-5} N/m².

Each sound pressure measurement was associated with the proper portion of the sphere surface area. It was assumed that the sound pressure levels on a circle around the array were typical of the levels on a sphere around the array with the array generating sound. The calculated sound power level was then subtracted from the sound level of an omnidirectional source which generates the same noise level as the array at $\alpha = 0^\circ$ (i.e., on the array axis).

Figure 10 shows that the calculated results agree fairly well with the measured values of noise rejection (data from fig. 8(h)). The differences between calculated and measured data were probably due to the wind tunnel test section being semireverberant rather than reverberant as assumed for the calculations.

CONCLUDING REMARKS

A four-element, digital-delay, end-fire microphone array was evaluated for use as a directional receiver in large wind tunnels. The array directivity measured in an anechoic chamber, though modest, agreed with theoretical predictions. The best directivity was attained with the ratio of microphone spacing to acoustic wave length, d/λ , kept between 0.35 and 0.88.

Despite the limited directivity of a four-element array, the device rejected 5 to 12 dB of reverberation and background noise (400-10,000 Hz) in the Ames 40- by 80-Foot Wind Tunnel. Rejection was good with and without forward speed over a range of d/λ from 0.18 to 3.53. Limited data indicated that the array measured approximately free-field noise levels of a horn driver 6.7 m (22 ft) away. It is estimated that the array will measure 6 dB less wind noise than would an omnidirectional microphone.

Although the array performance in the wind tunnel was much better than that of an omnidirectional receiver, longer arrays with more element are needed to achieve necessary directivity and low frequency discrimination.

REFERENCES

1. Kraus, John D.: Antennas. McGraw-Hill, New York, 1950.
2. Collin, Robert E. and Zucker, Francis J.: Antenna Theory, Part I. McGraw-Hill, New York, 1969.
3. Pritchard, R. L.: Optimum Directivity Patterns for Linear Arrays. Acoustics Res. Lab. Tech. Memo. No. 7 (1950), Harvard University.
4. Berkta, H. O. and Shooter, J. A.: Nearfield Effects In End-Fire Line Arrays. J. Acoust. Soc. Amer. 53, 550-563 (1973).
5. Groves, I. D., Jr. and Benedetti, V. P.: Acoustic Measurements with a Circular Nearfield Array in an Anechoic Water-Filled Tank. JASA Vol. 54, No. 3, Sept. 1973.
6. Tatge, R. B.: Directive Acoustic Arrays For Jet-Engine Noise Source Localization. Report No. 70-C-052, General Electric, Schenectady, New York, Jan. 1970.
7. El-Sum, H. M. A. and Mawardi, O. K.: Diagnostic Techniques For Measurement of Aerodynamic Noise In Free Field and Reverberant Environment of Wind Tunnels. NASA CR 114636, May 1973.
8. Bies, David A.: Investigation of the Feasibility of Making Model Acoustic Measurements in the NASA Ames 40- by 80-Foot Wind Tunnel. NASA CR-114352, July 1971.
9. Noiseux, D. U.: Study of Porous Surface Microphones For Acoustic Measurements In Wind Tunnels. NASA CR 114593, April 1973.
10. Beranek, Leo L., ed.: Noise and Vibration Control. McGraw-Hill Book Company, 1971.

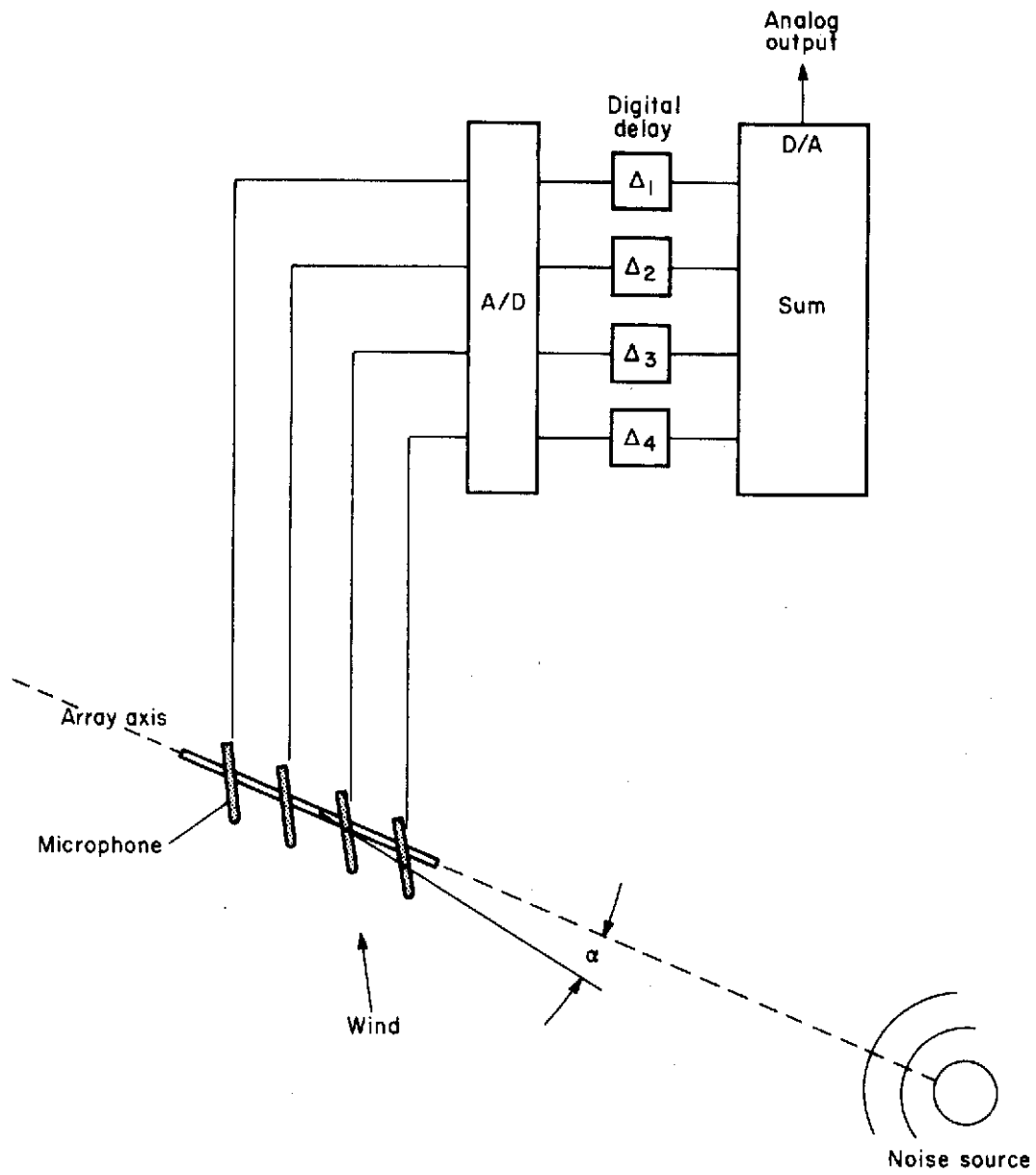
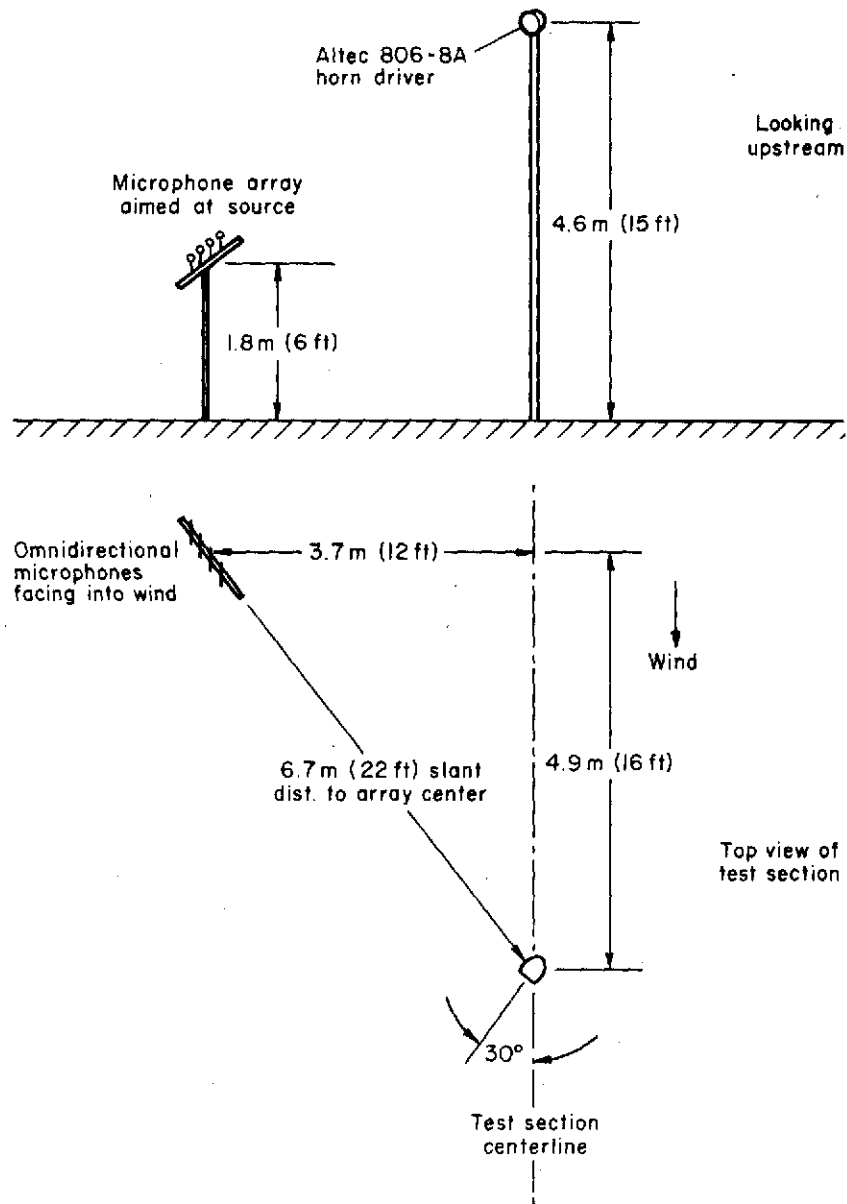
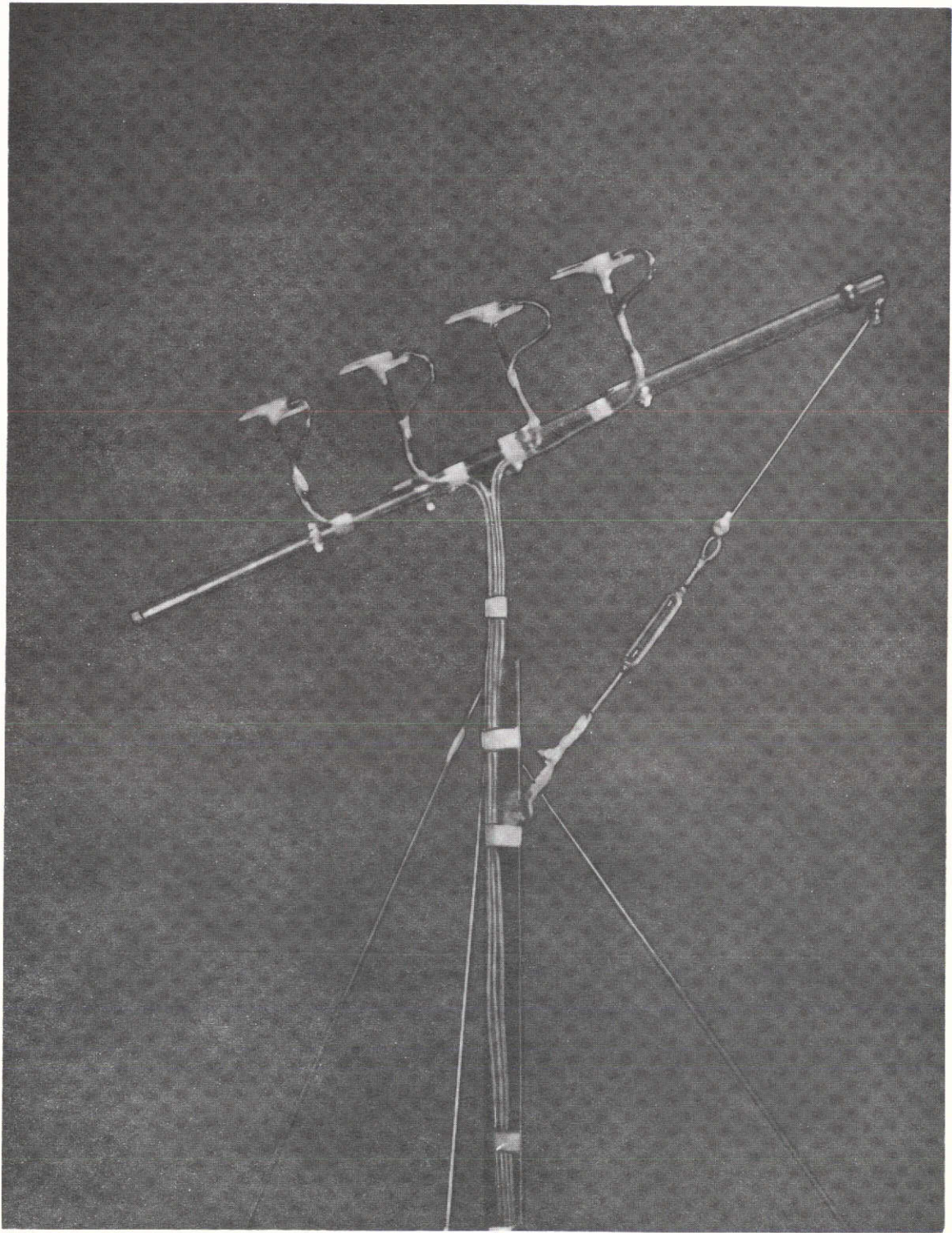


Figure 1.— End-fire, phased array of microphones.



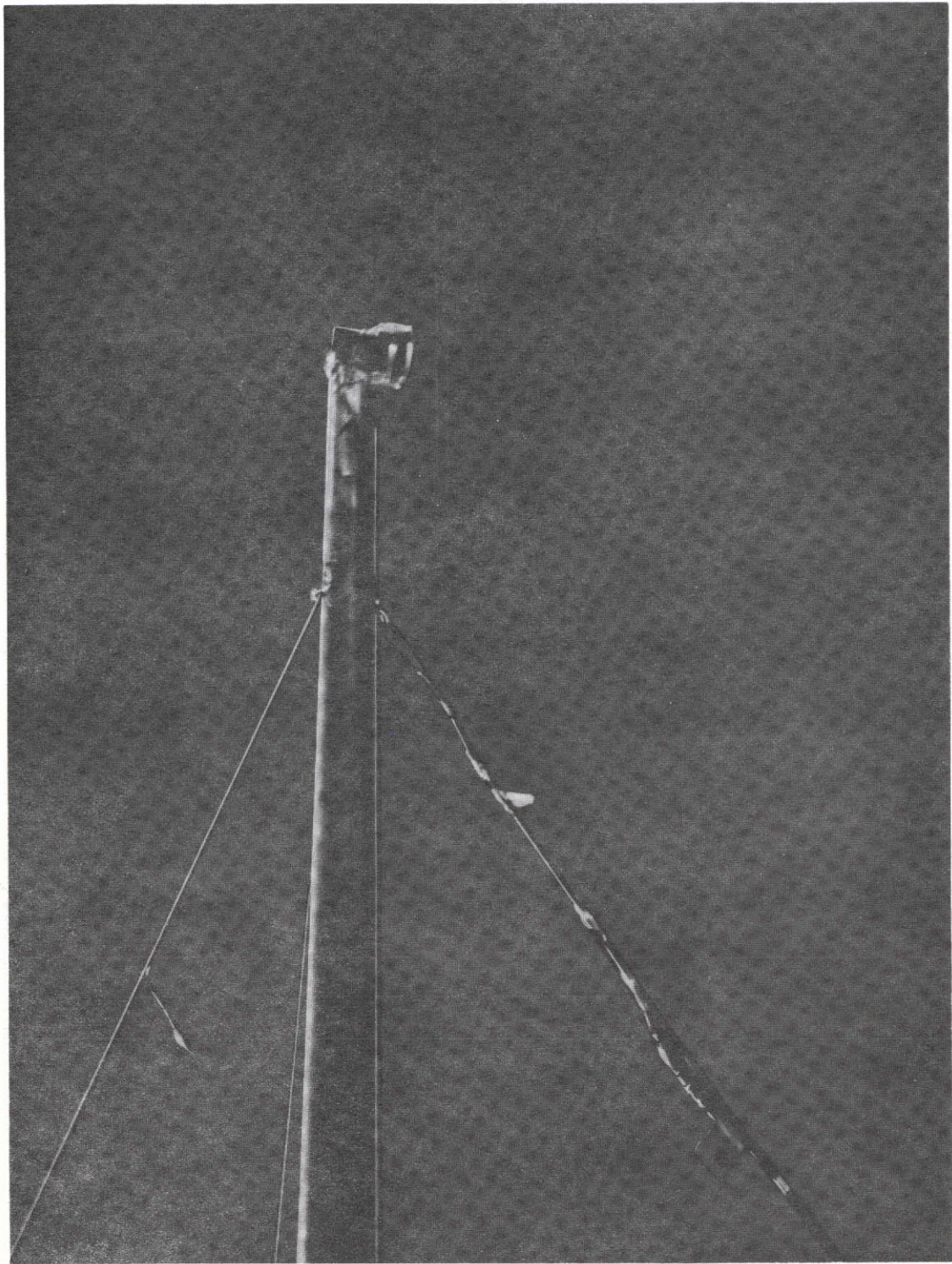
(a) Schematic.

Figure 2.— End-fire array and loudspeaker in 40- by 80-foot wind tunnel test section.



(b) Photograph of array.

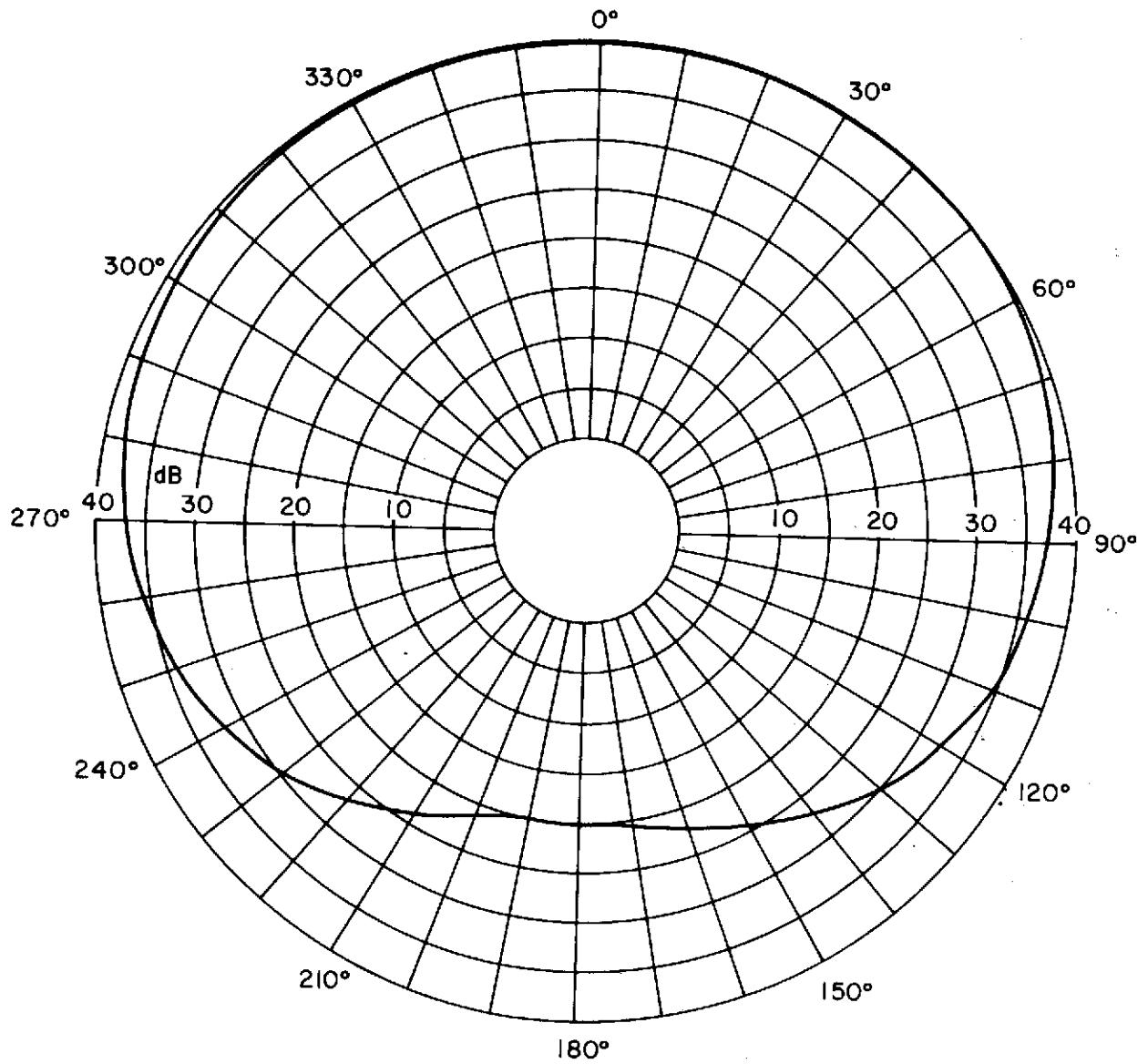
Figure 2.— Continued.



(c) Photograph of source.

Figure 2.— Concluded.

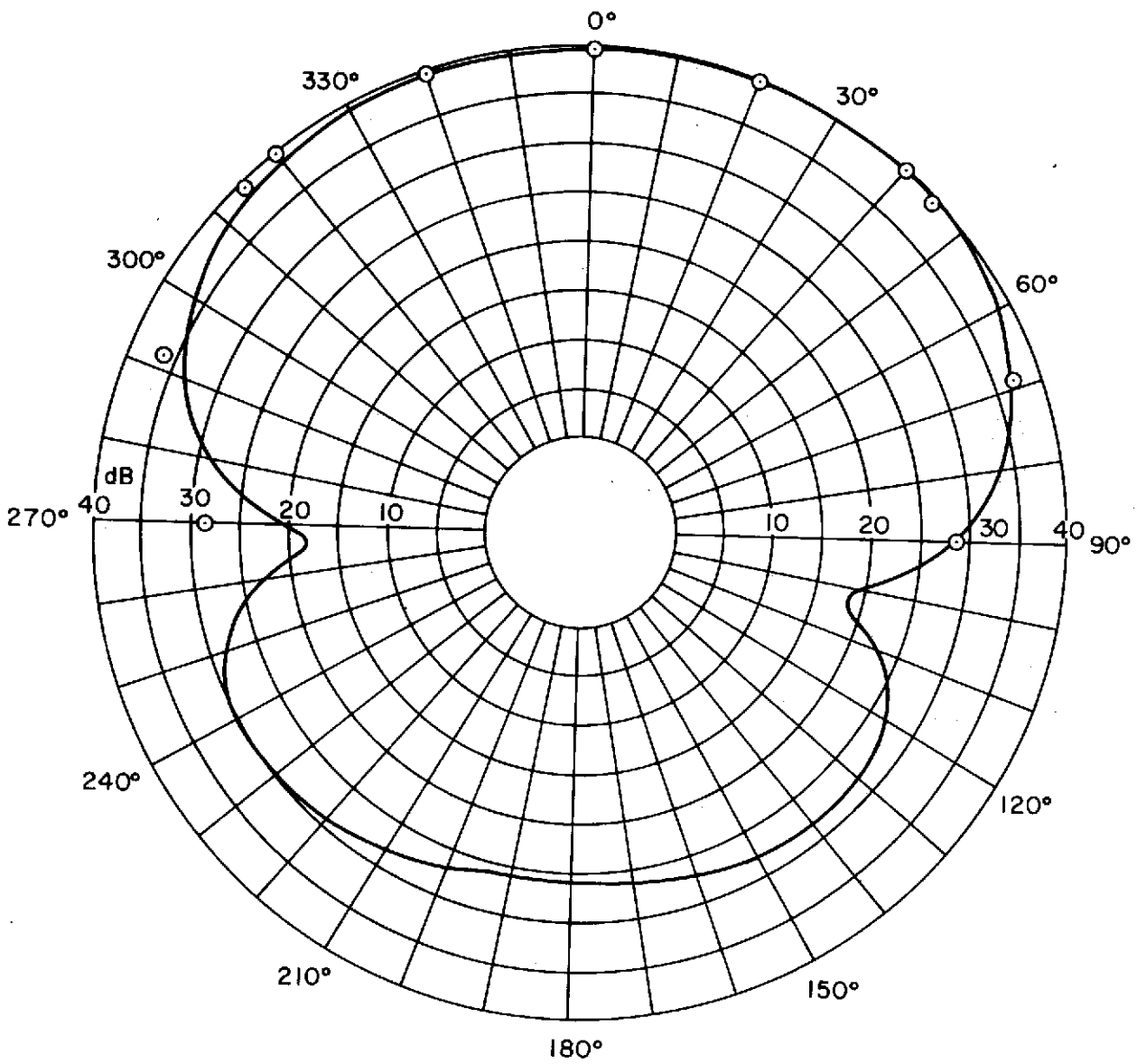
250 Hz 15 cm (1/2 ft) spacing



(a) $d/\lambda = 0.11$

Figure 3.— Directivity pattern of four-element array with uniform spacing. Tone source. Directivity angle is relative to array axis.

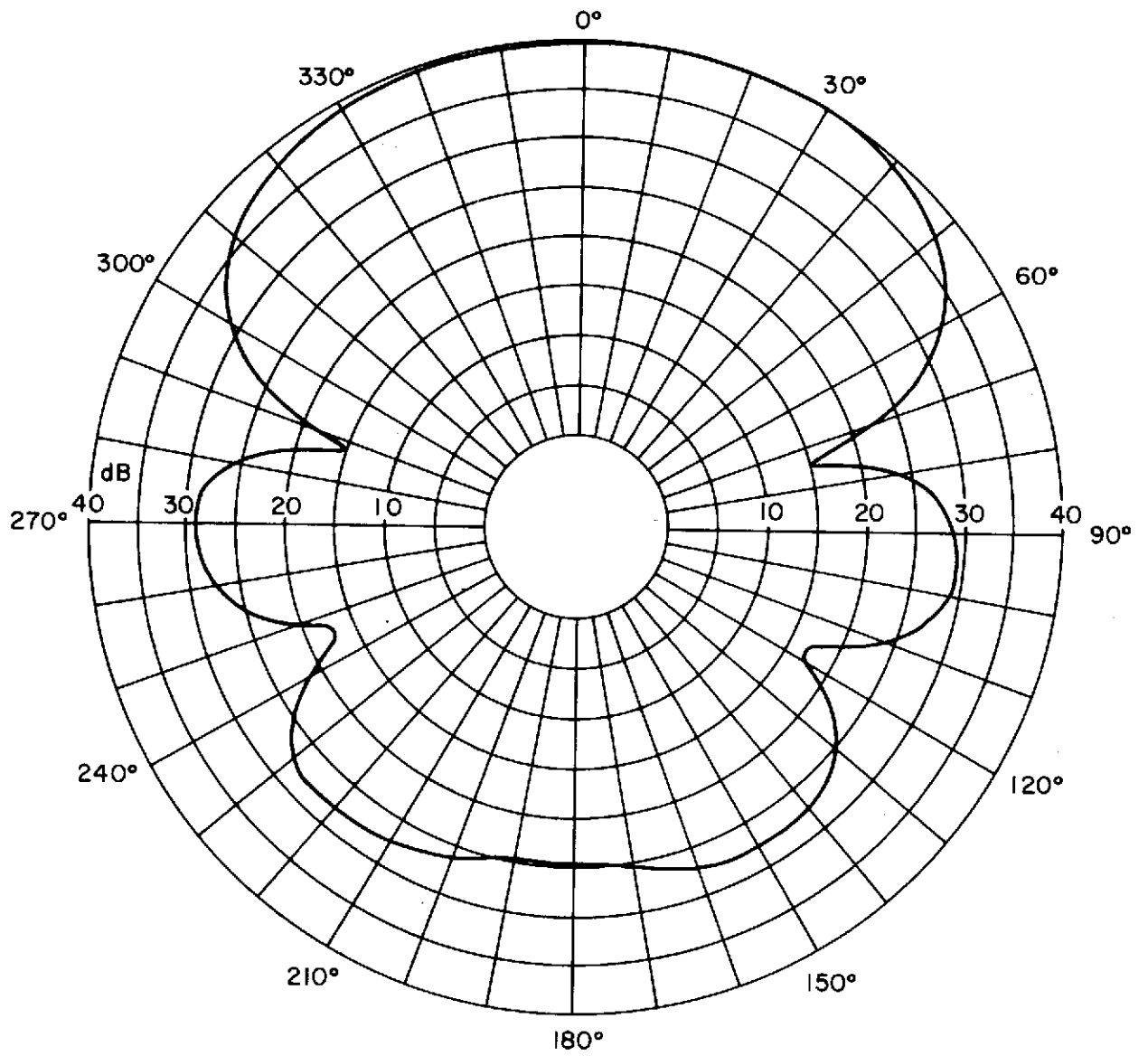
○ Theory
— Experiment
500 Hz 15 cm (1/2 ft) spacing



(b) $d/\lambda = 0.22$

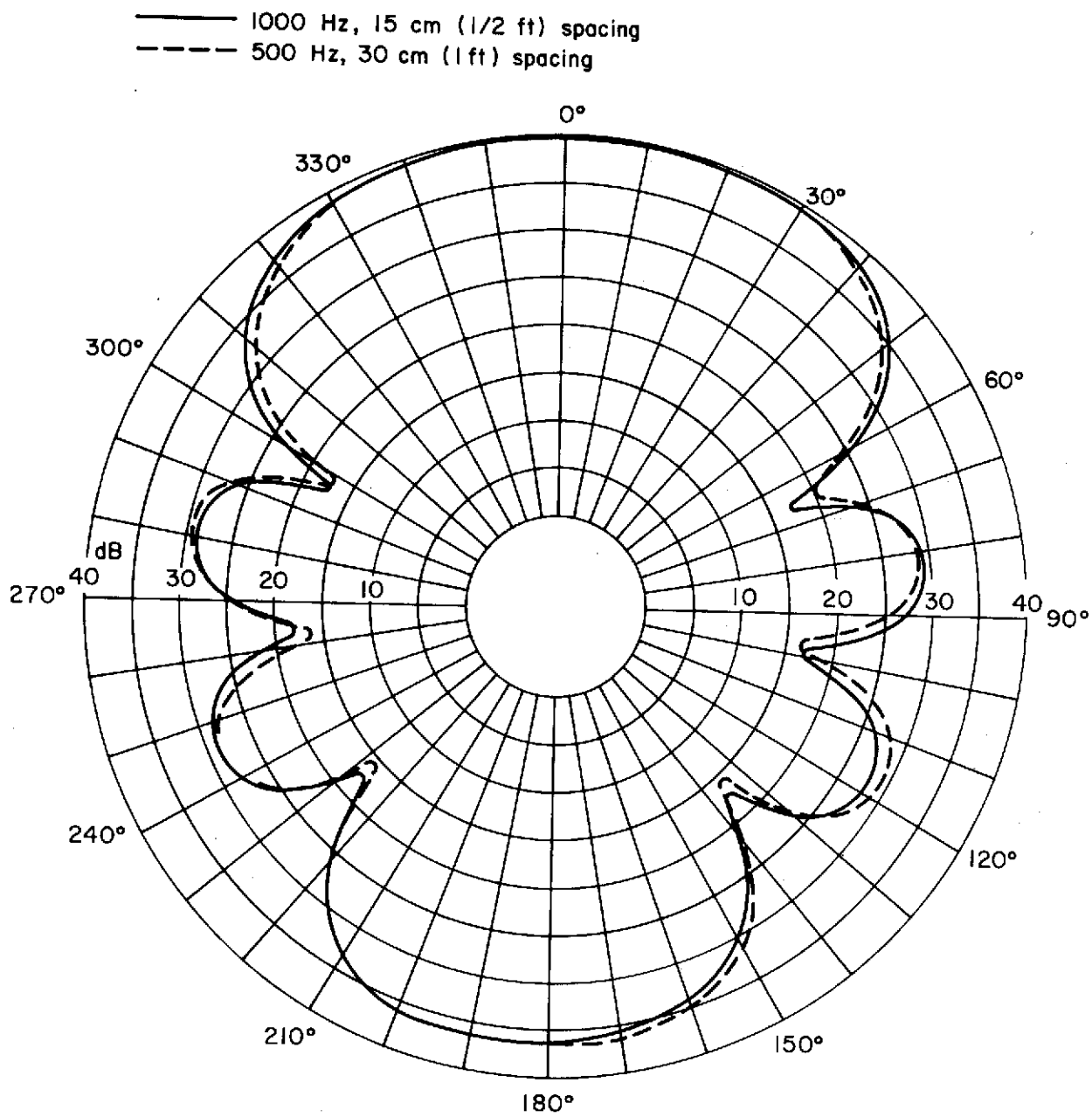
Figure 3.— Continued.

800 Hz 15 cm (1/2 ft) spacing



(c) $d/\lambda = 0.35$

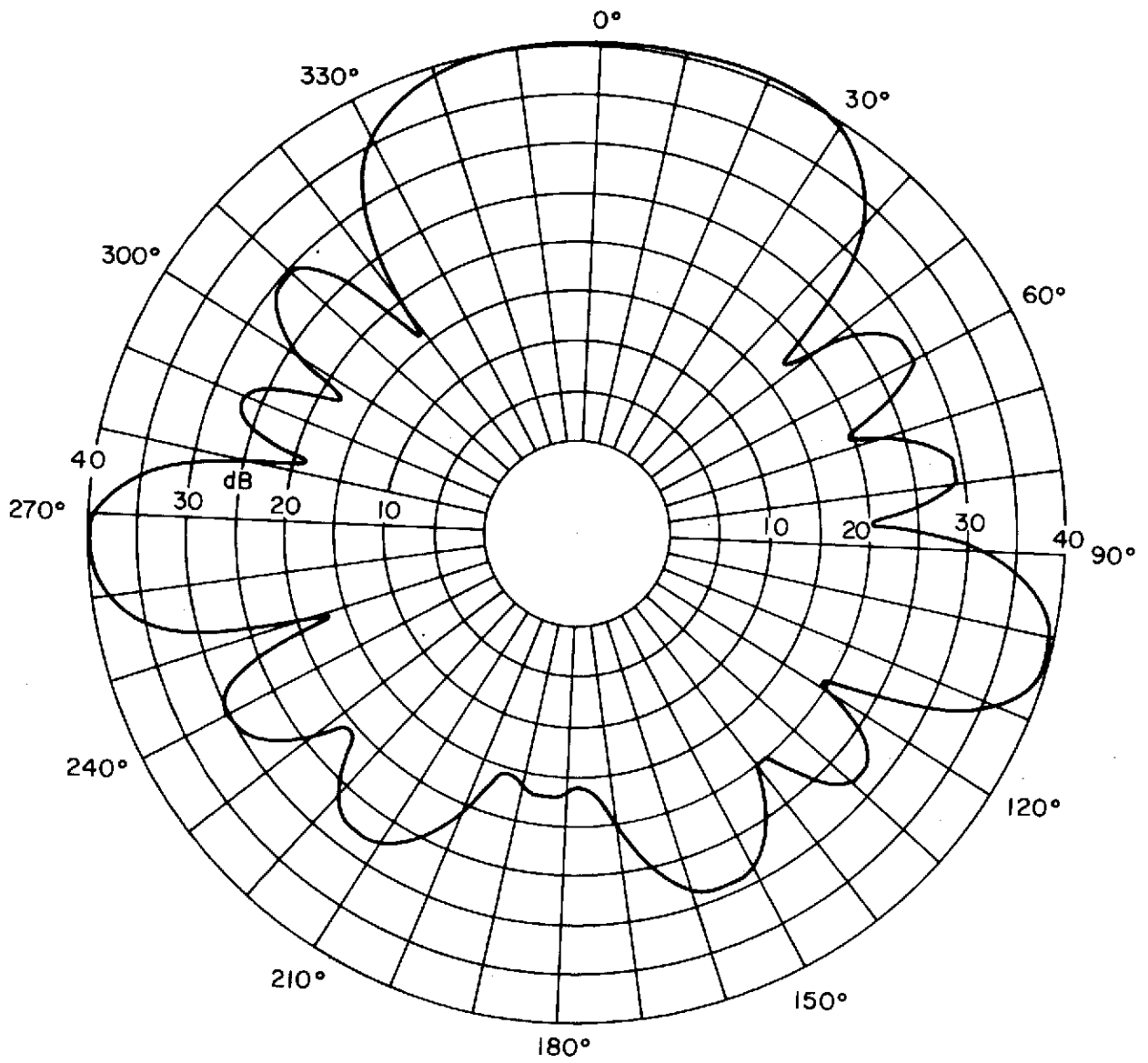
Figure 3.— Continued.



(d) $d/\lambda = 0.44$

Figure 3.— Continued.

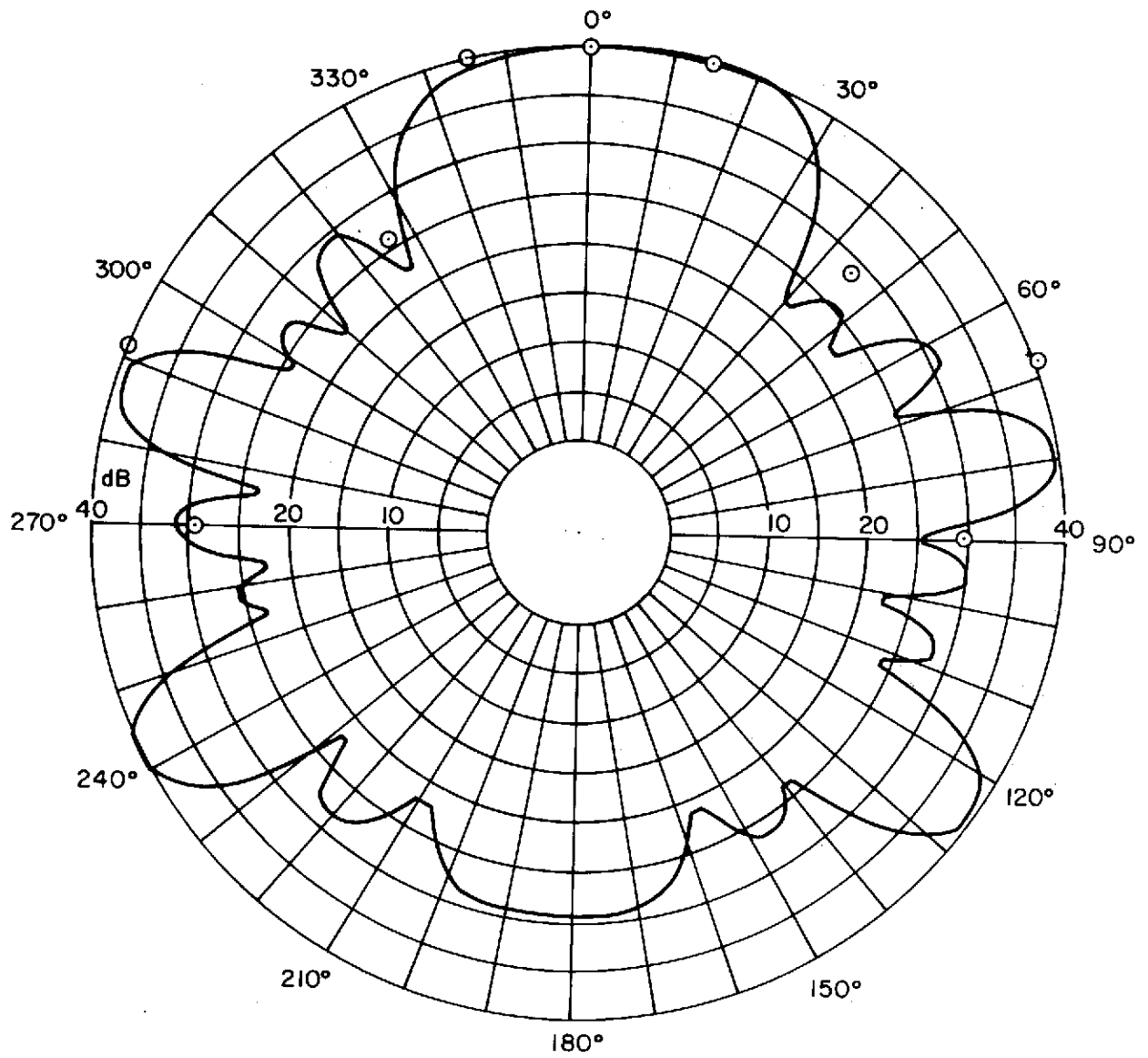
2000 Hz 15 cm (1/2 ft) spacing



(e) $d/\lambda = 0.88$

Figure 3.— Continued.

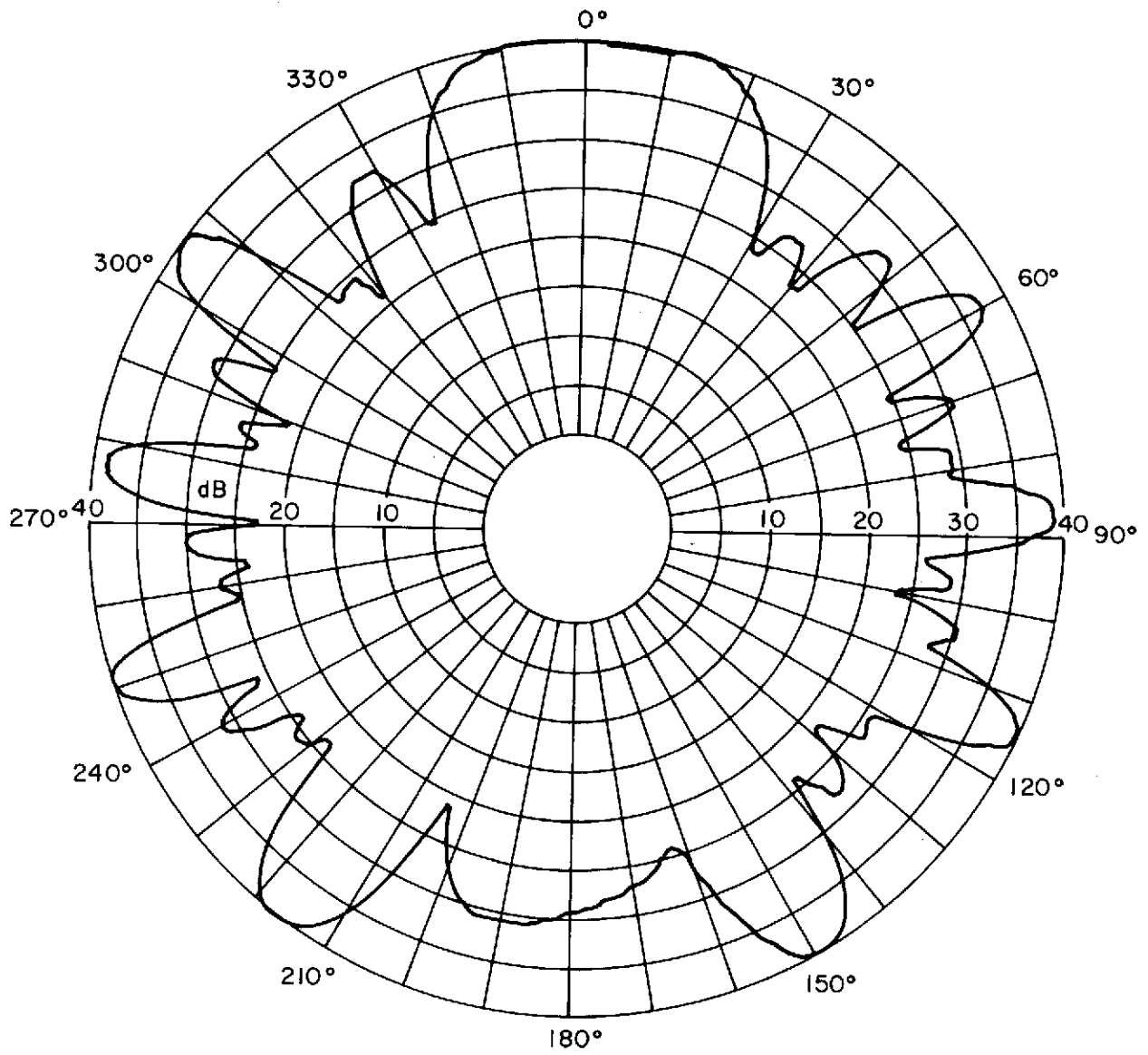
○ Theory
— Experiment
3000 Hz 15 cm (1/2 ft) spacing



(f) $d/\lambda = 1.33$

Figure 3.— Continued.

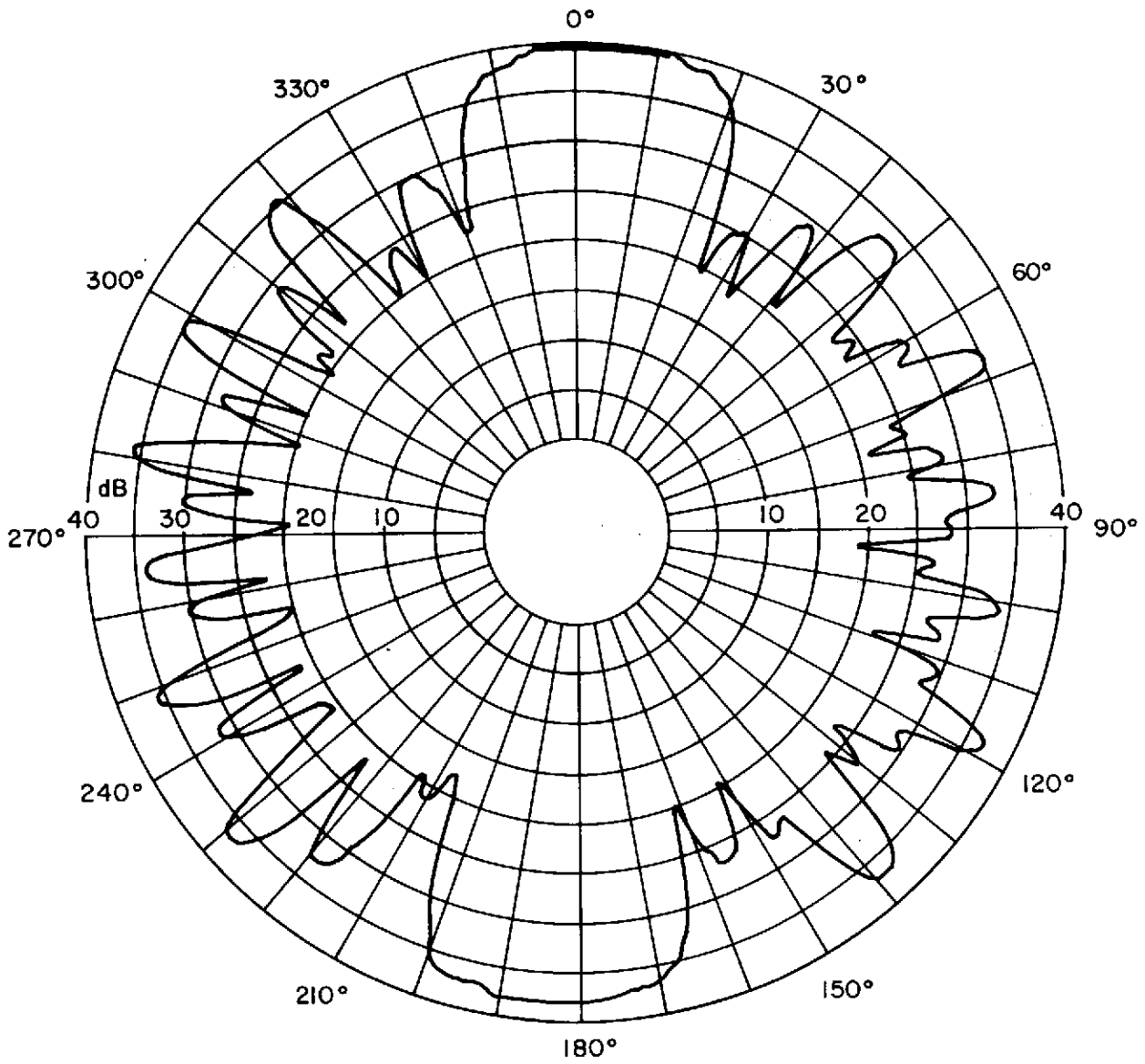
5000 Hz 15 cm (1/2 ft) spacing



(g) $d/\lambda = 2.22$

Figure 3.— Continued.

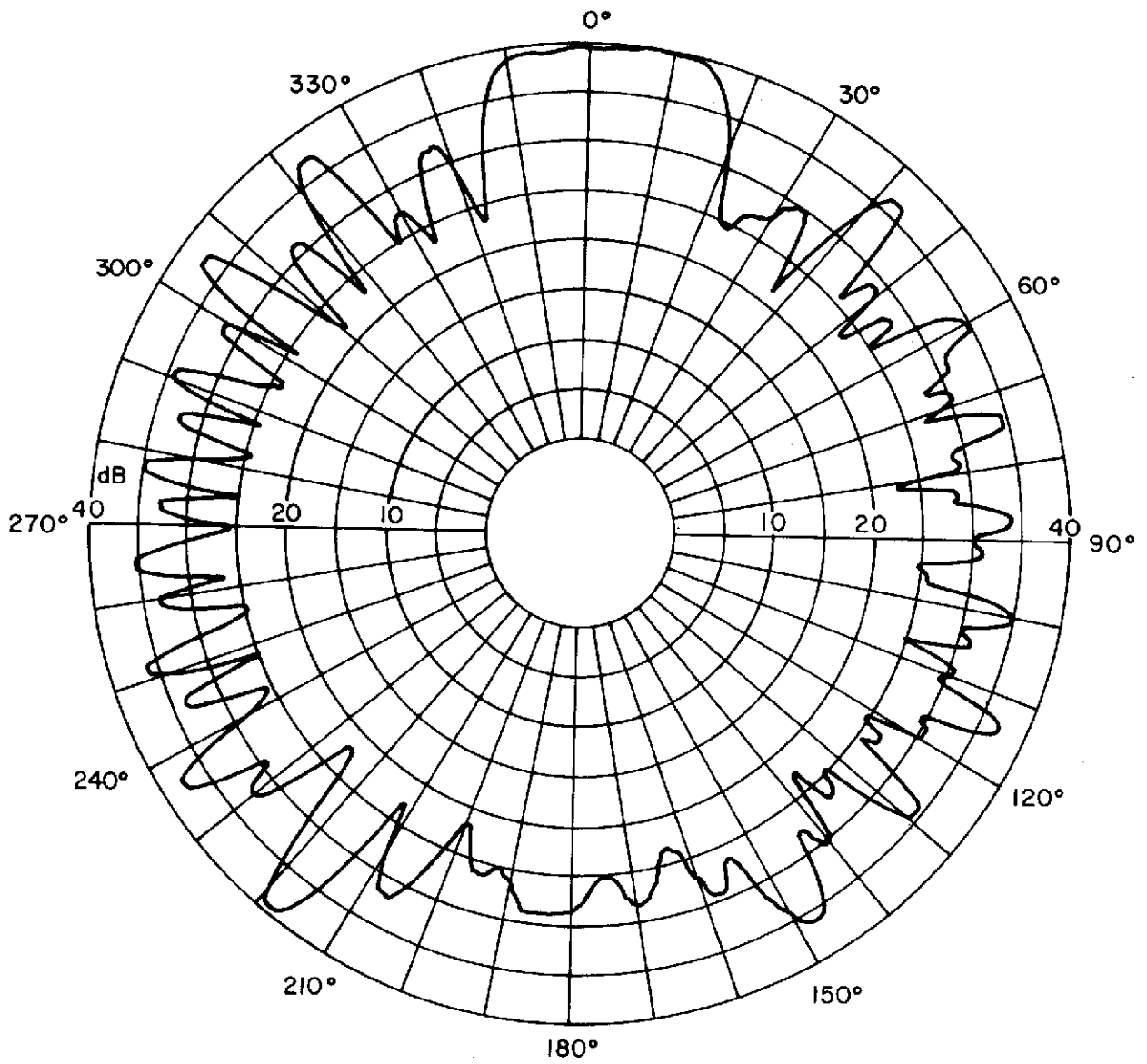
8000 Hz 15 cm (1/2 ft) spacing



(h) $d/\lambda = 3.54$

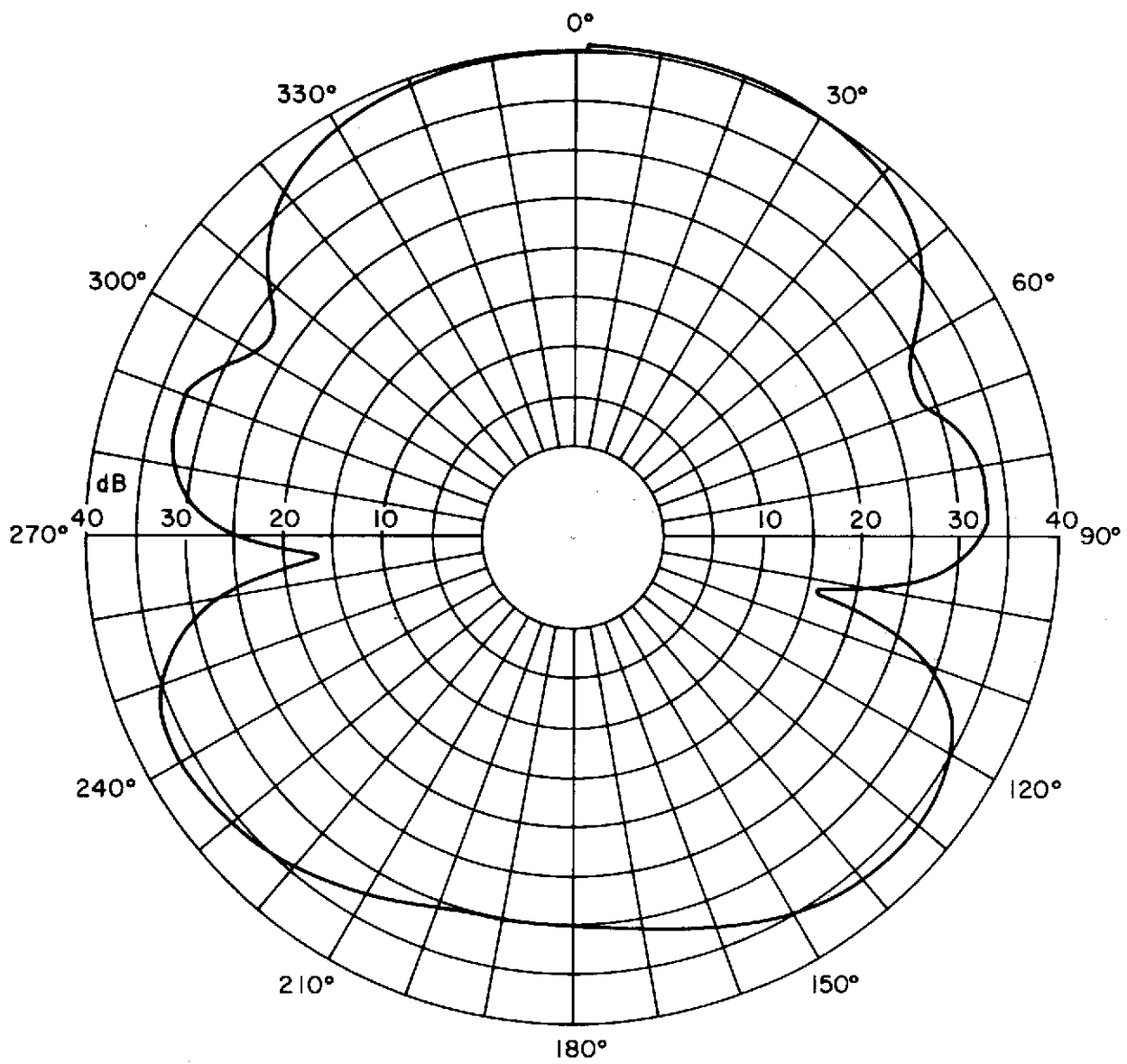
Figure 3.— Continued.

10,000 Hz 15 cm (1/2 ft) spacing



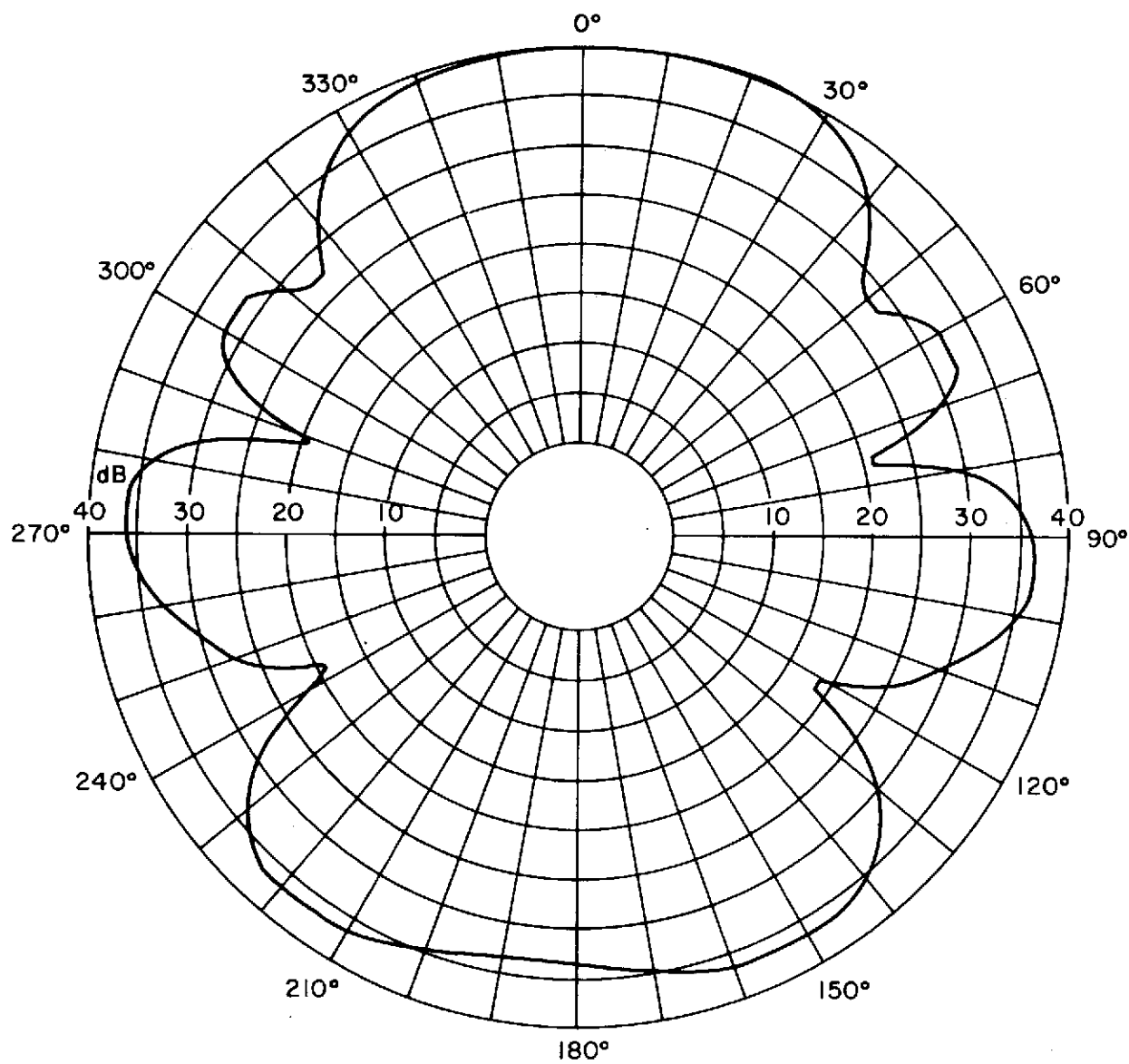
(i) $d/\lambda = 4.43$

Figure 3.— Concluded.



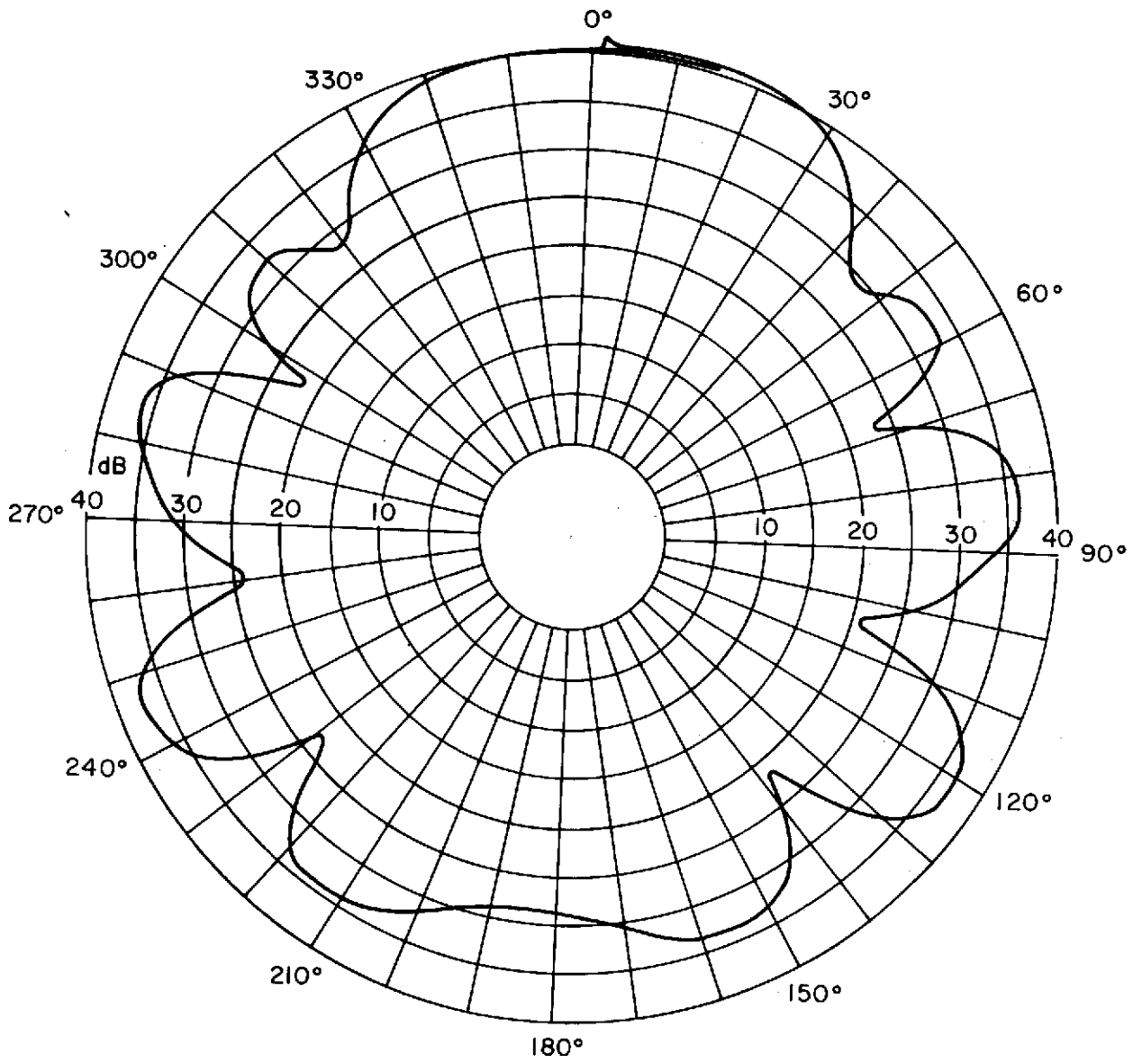
(a) 500 Hz tone.

Figure 4.— Directivity pattern of array with nonuniform spacing of 15, 30 and 46 centimeters (0.5, 1.0, and 1.5 ft), respectively, between microphones.



(b) 800 Hz tone.

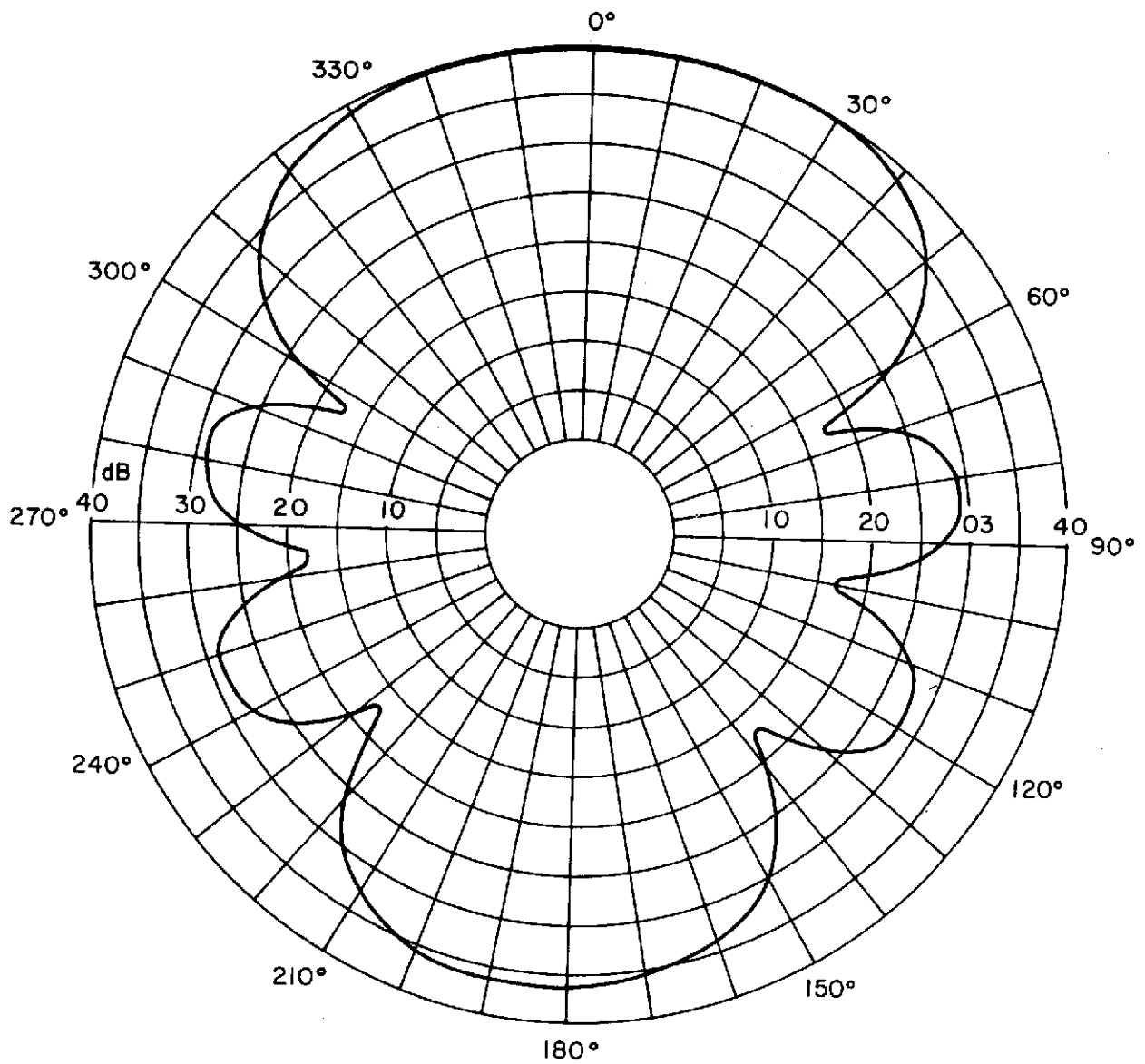
Figure 4.— Continued.



(c) 1000 Hz tone.

Figure 4.— Concluded.

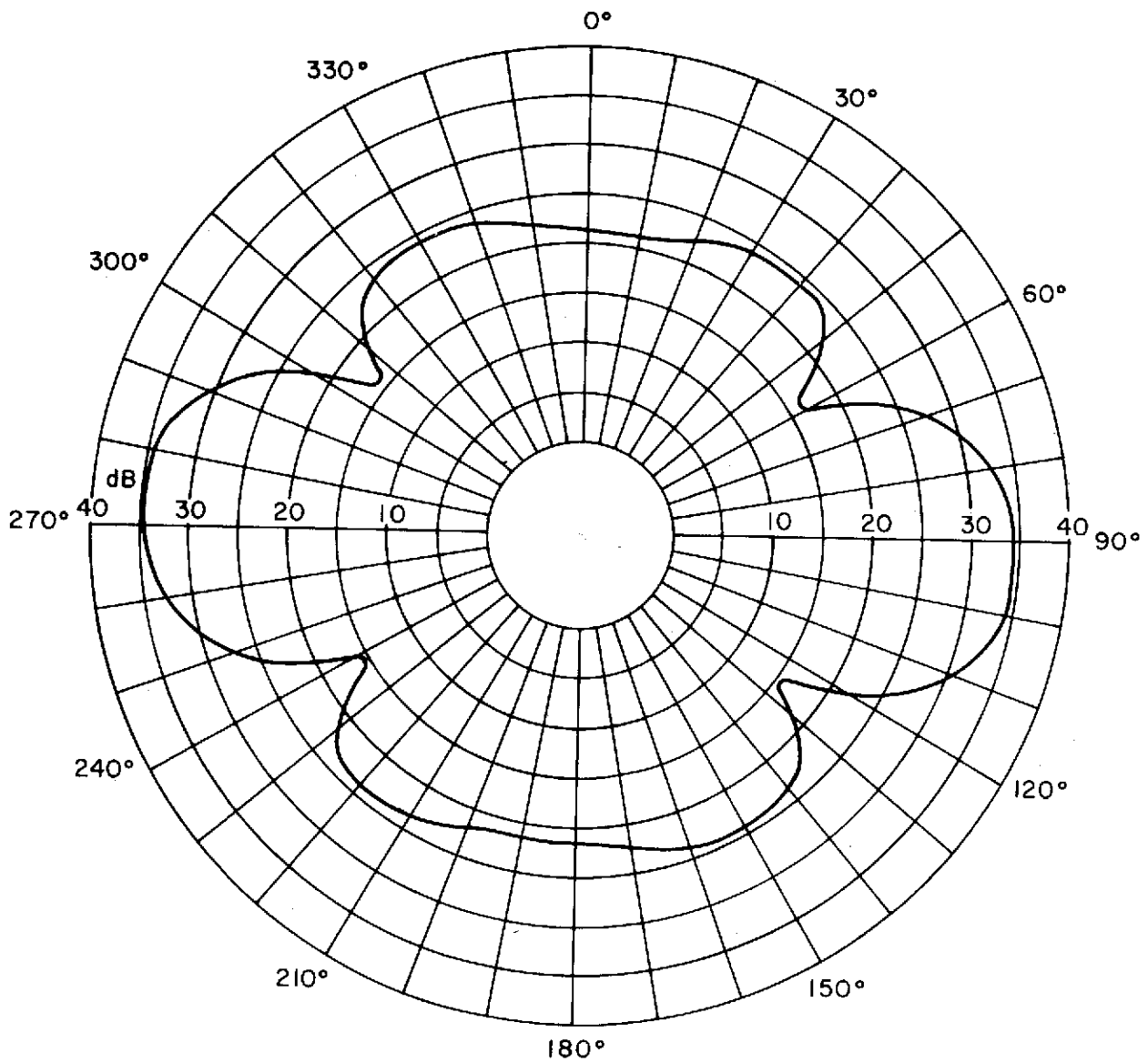
1000 Hz 15 cm (1/2 ft) spacing
 $d/\lambda = 0.44$



(a) End-fire.

Figure 5.— Comparison of end-fire directivity with broad-side (no delay).
Tone source.

1000 Hz, 15 cm (1/2 ft) spacing
 $d/\lambda = 0.44$



(b) Broad-side.

Figure 5.— Concluded.

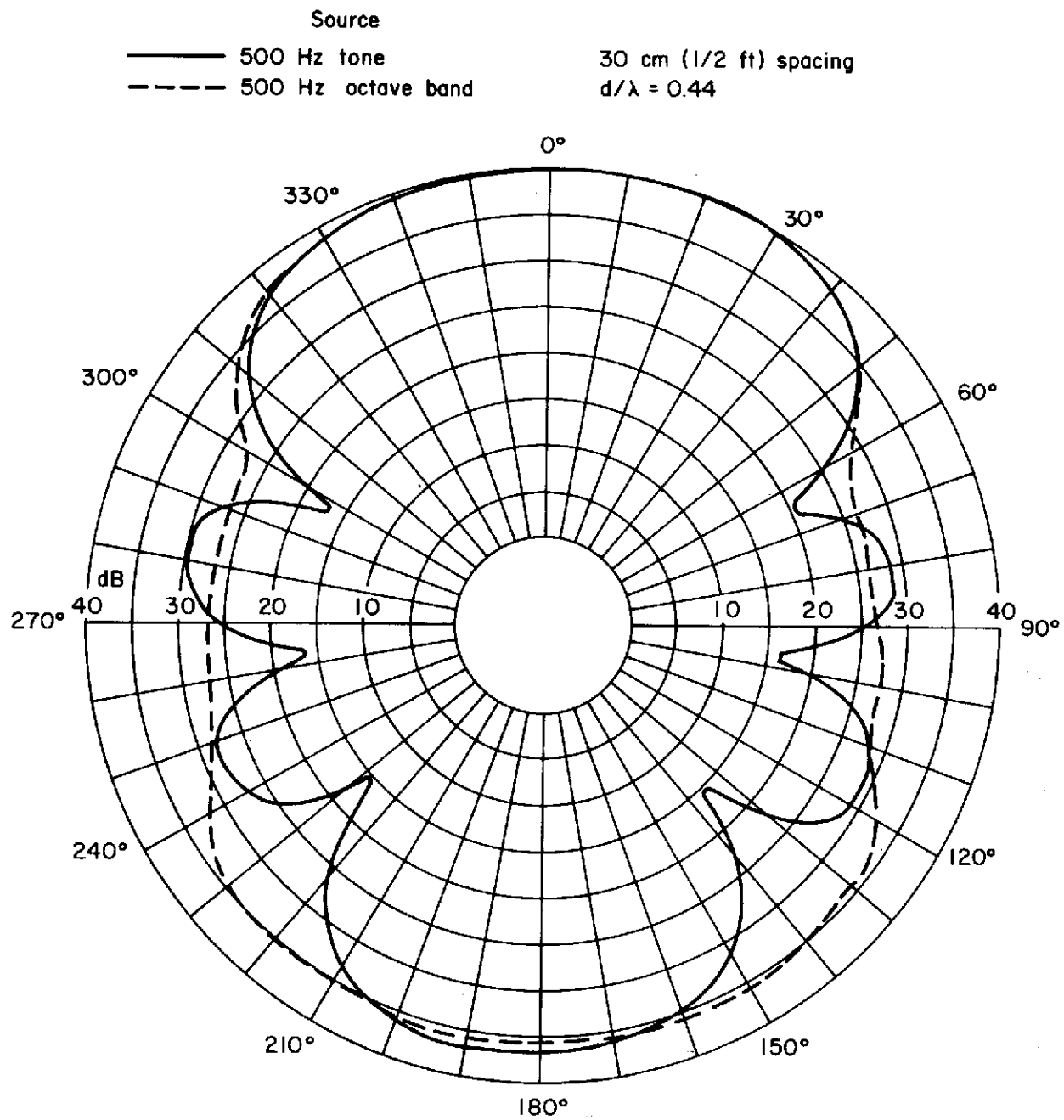
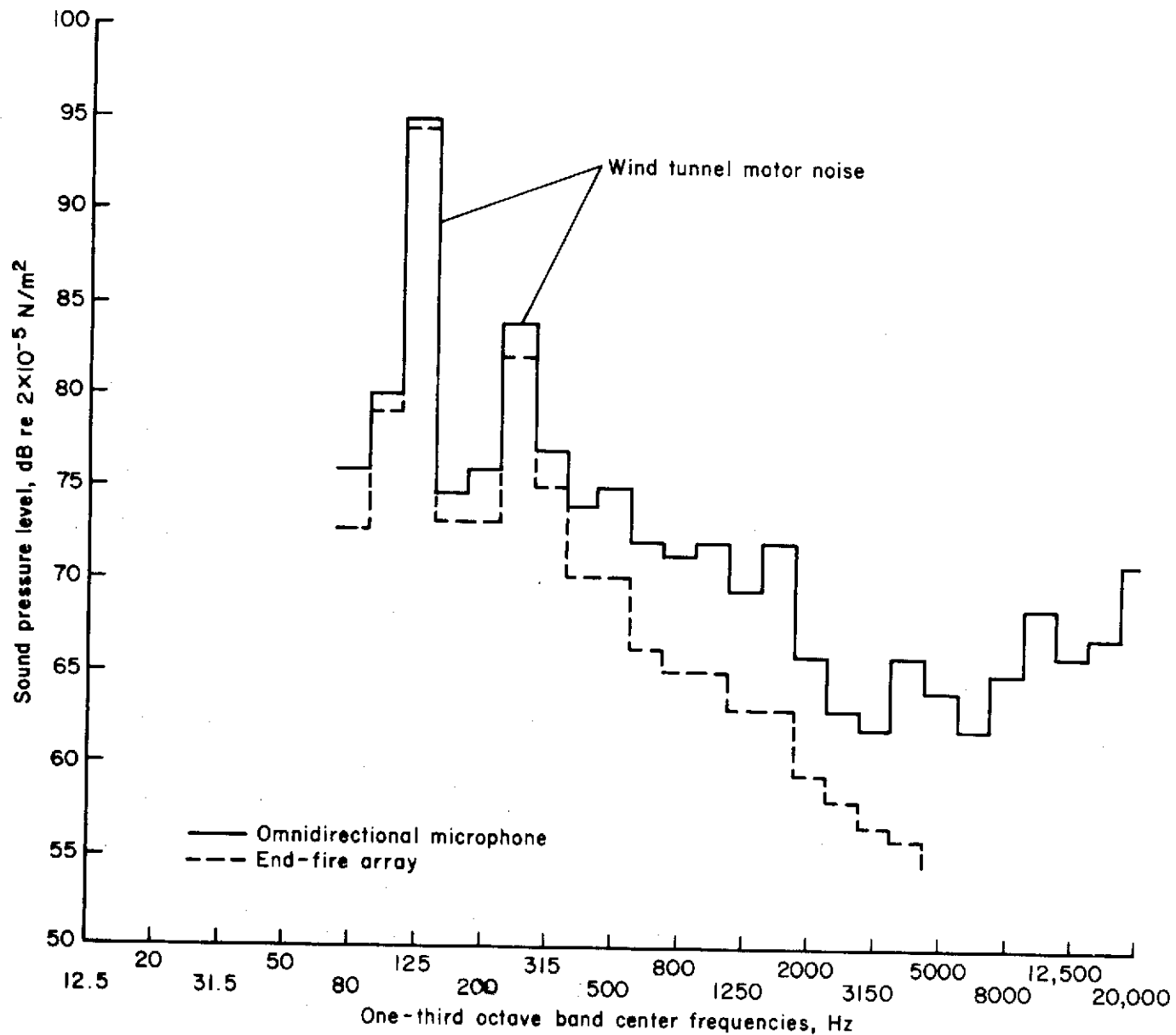
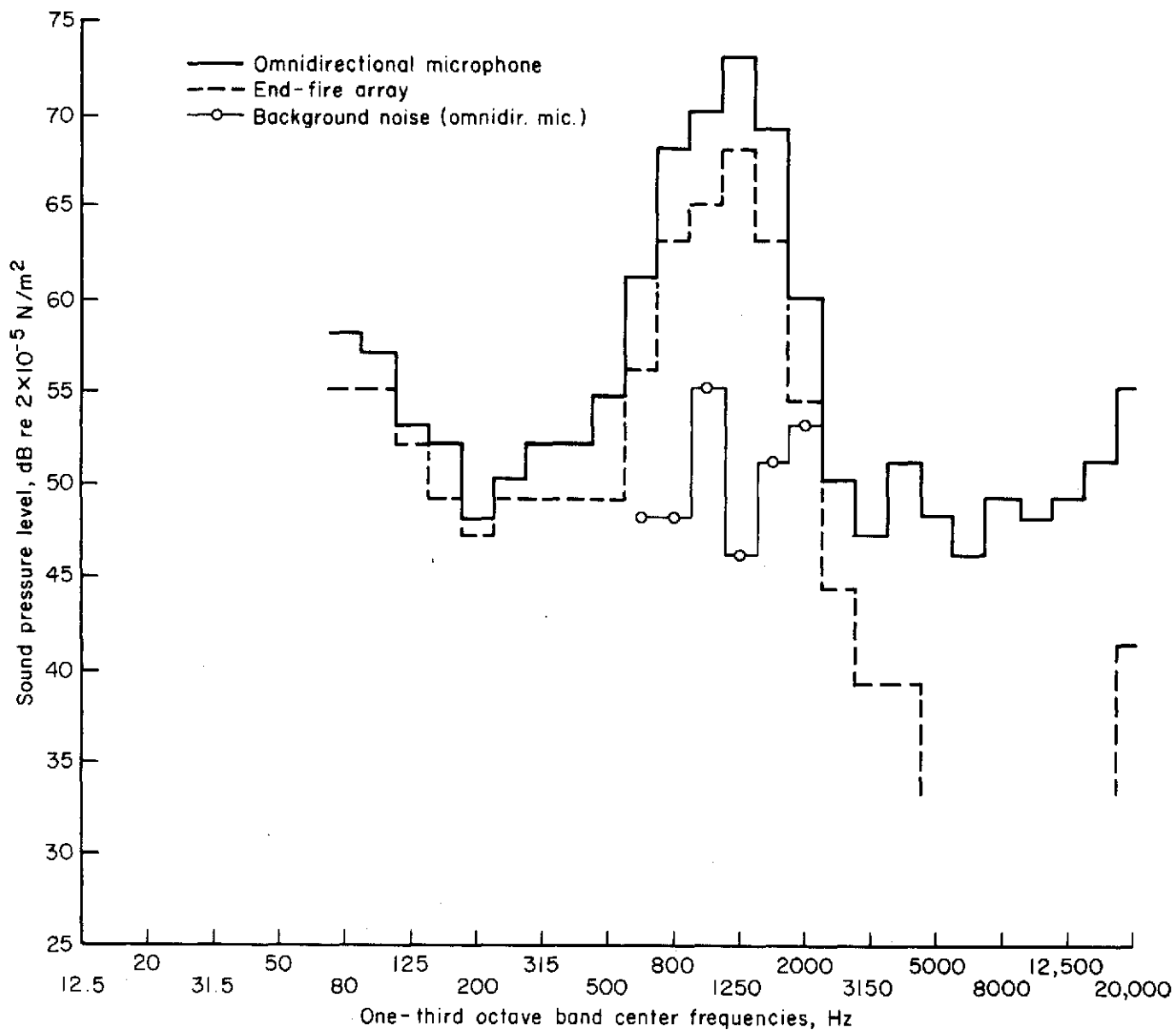


Figure 6.— Effect of random noise in an octave band.



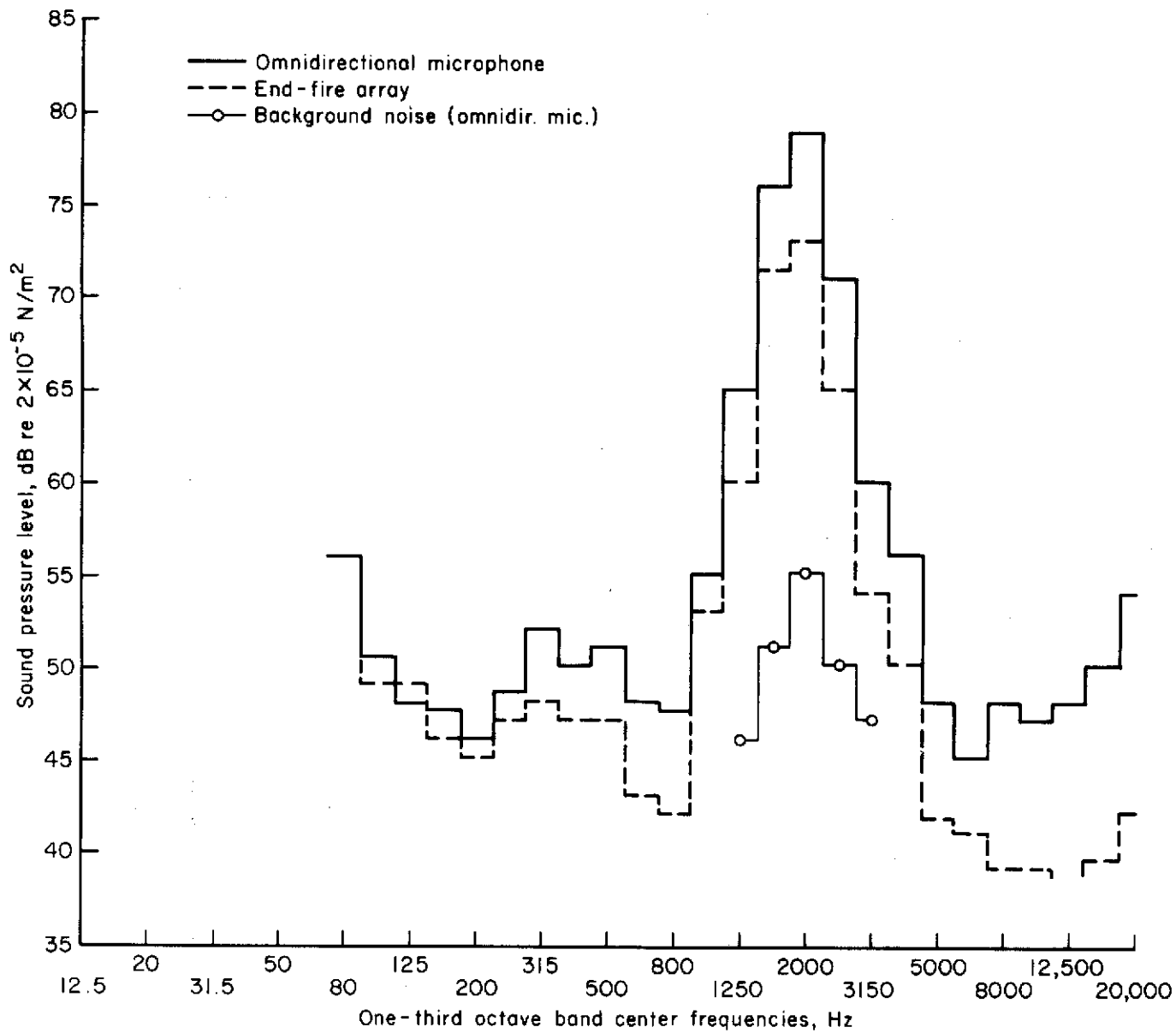
(a) Horn off, $U = 18$ m/s (58 f/s), background noise.

Figure 7.— Comparison of end-fire response with omnidirectional microphone response. Array spacing 15 cm (1/2 ft).



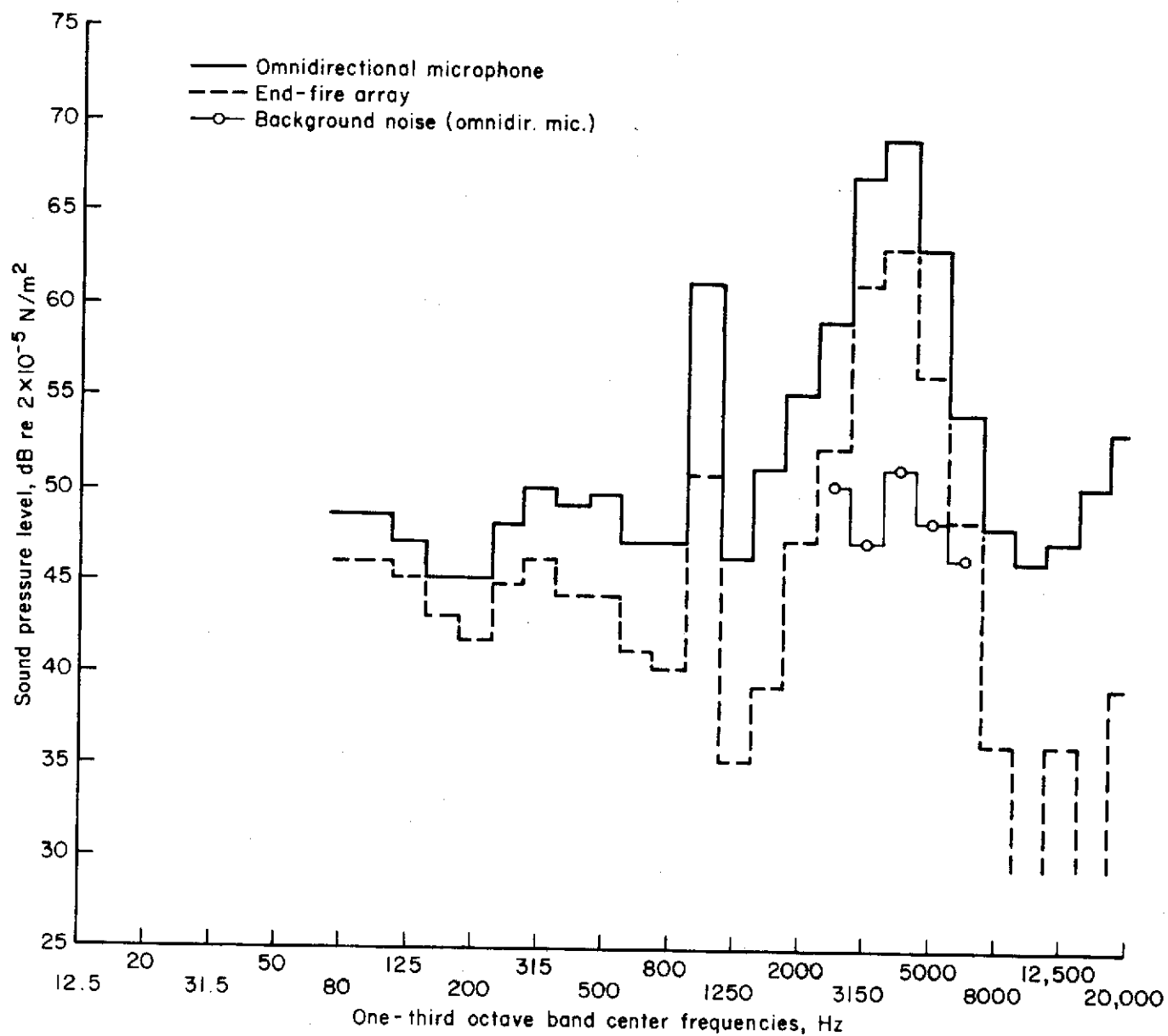
(b) $U = 0$, 1000 Hz octave band random (pink) noise from horn.

Figure 7.— Continued.



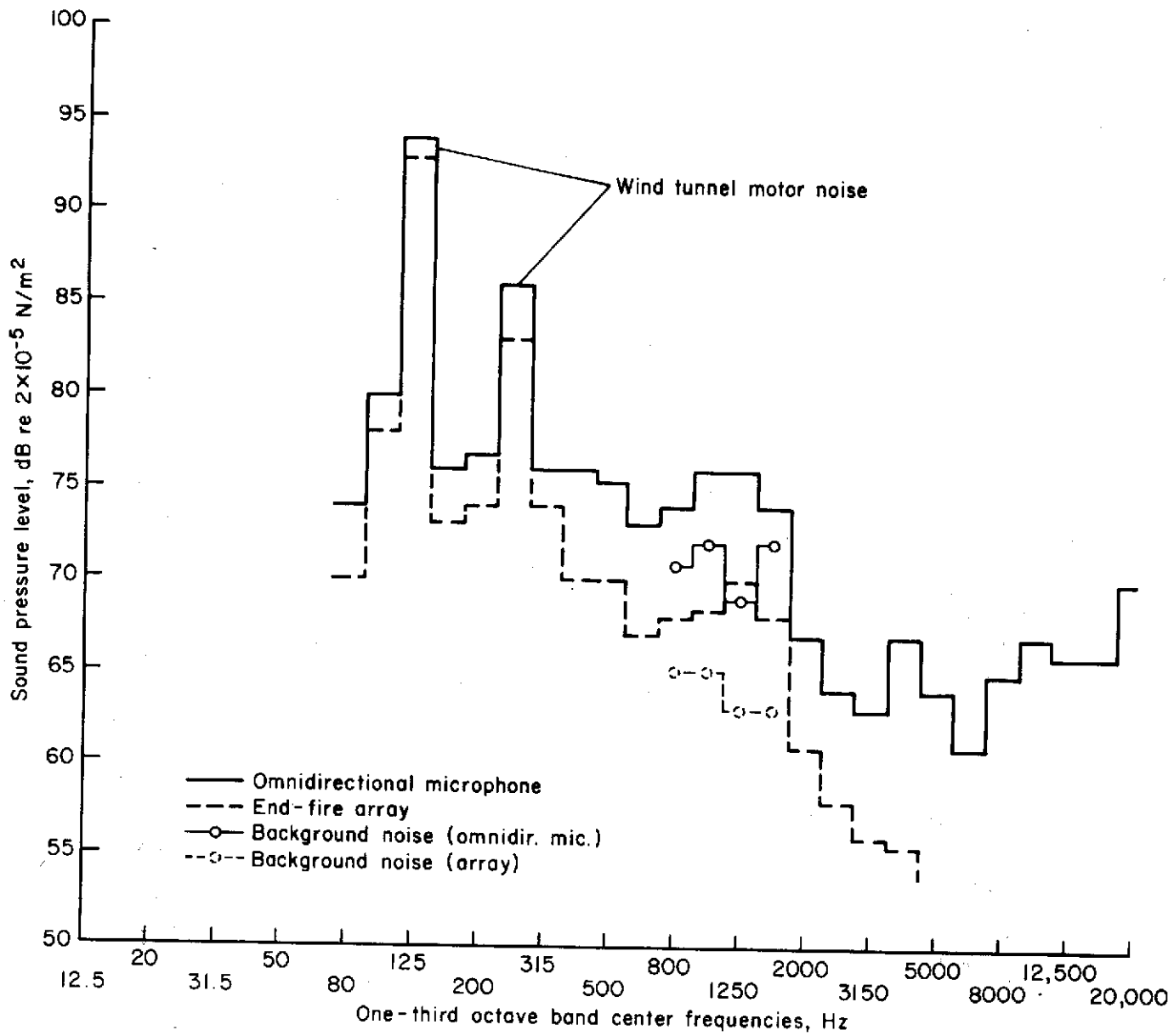
(c) $U = 0$, 2000 Hz.

Figure 7.— Continued.



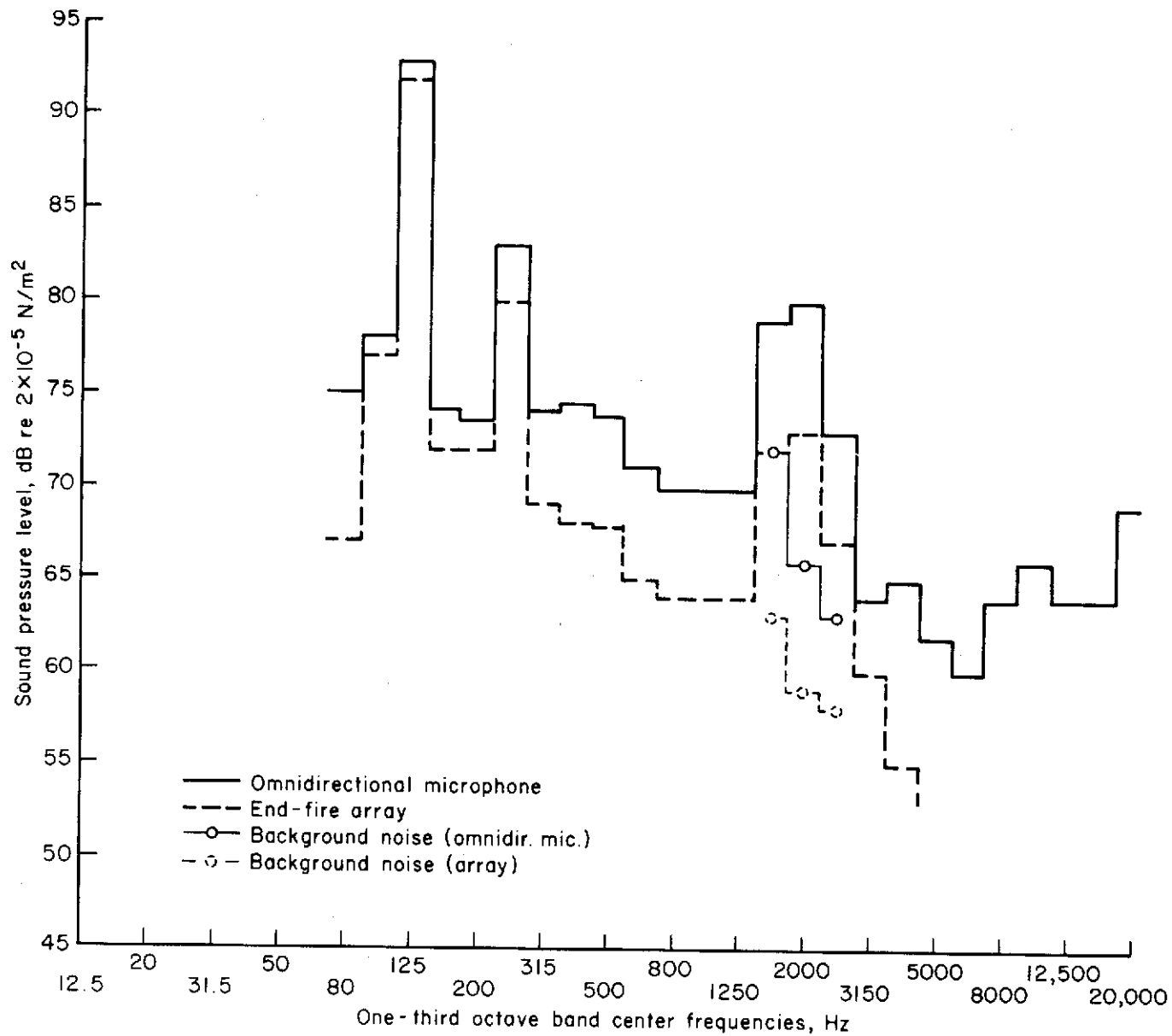
(d) $U = 0$, 4000 Hz.

Figure 7.— Continued.



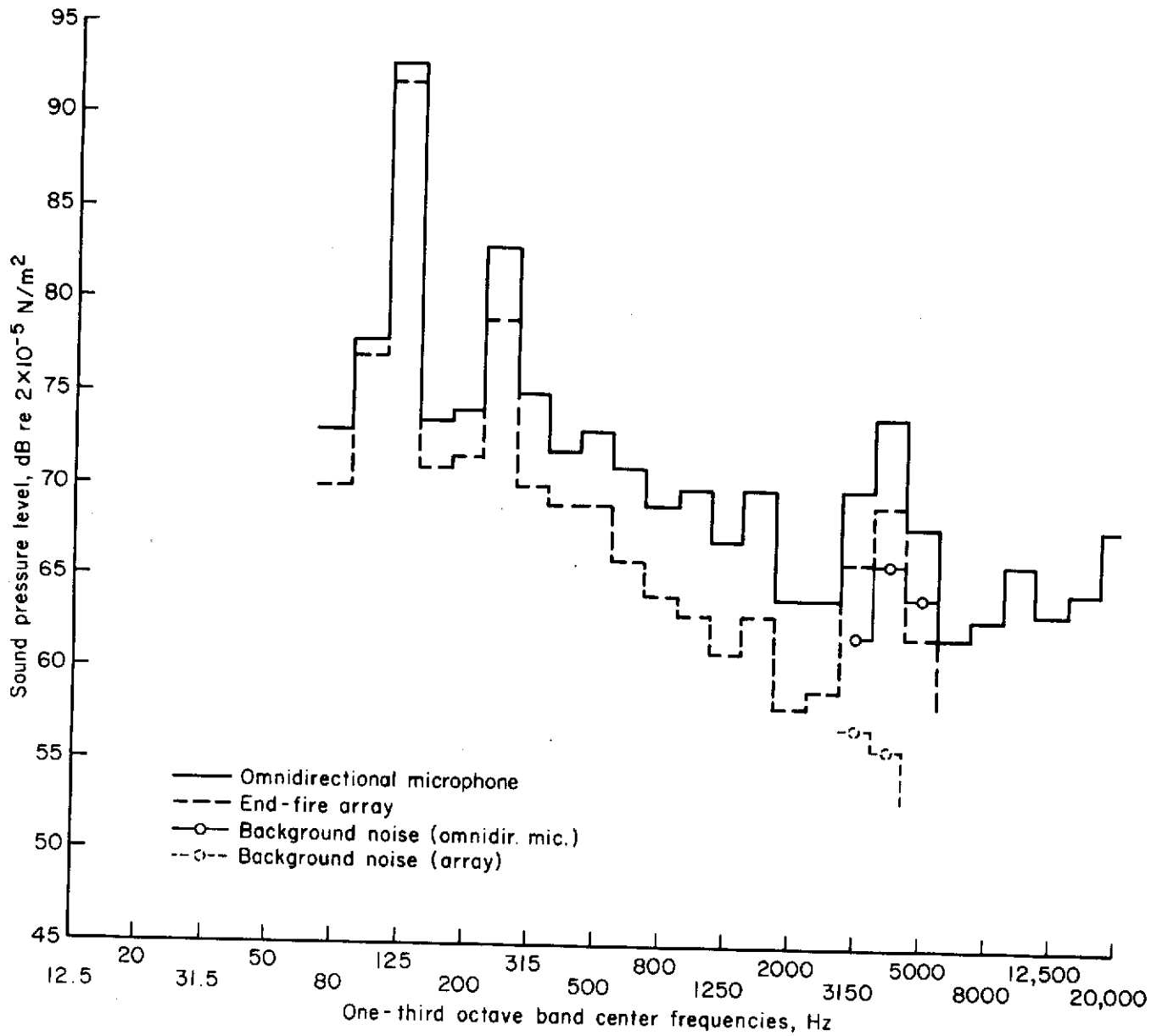
(e) $U = 18$ m/s (58 f/s), 1000 Hz.

Figure 7.— Continued.



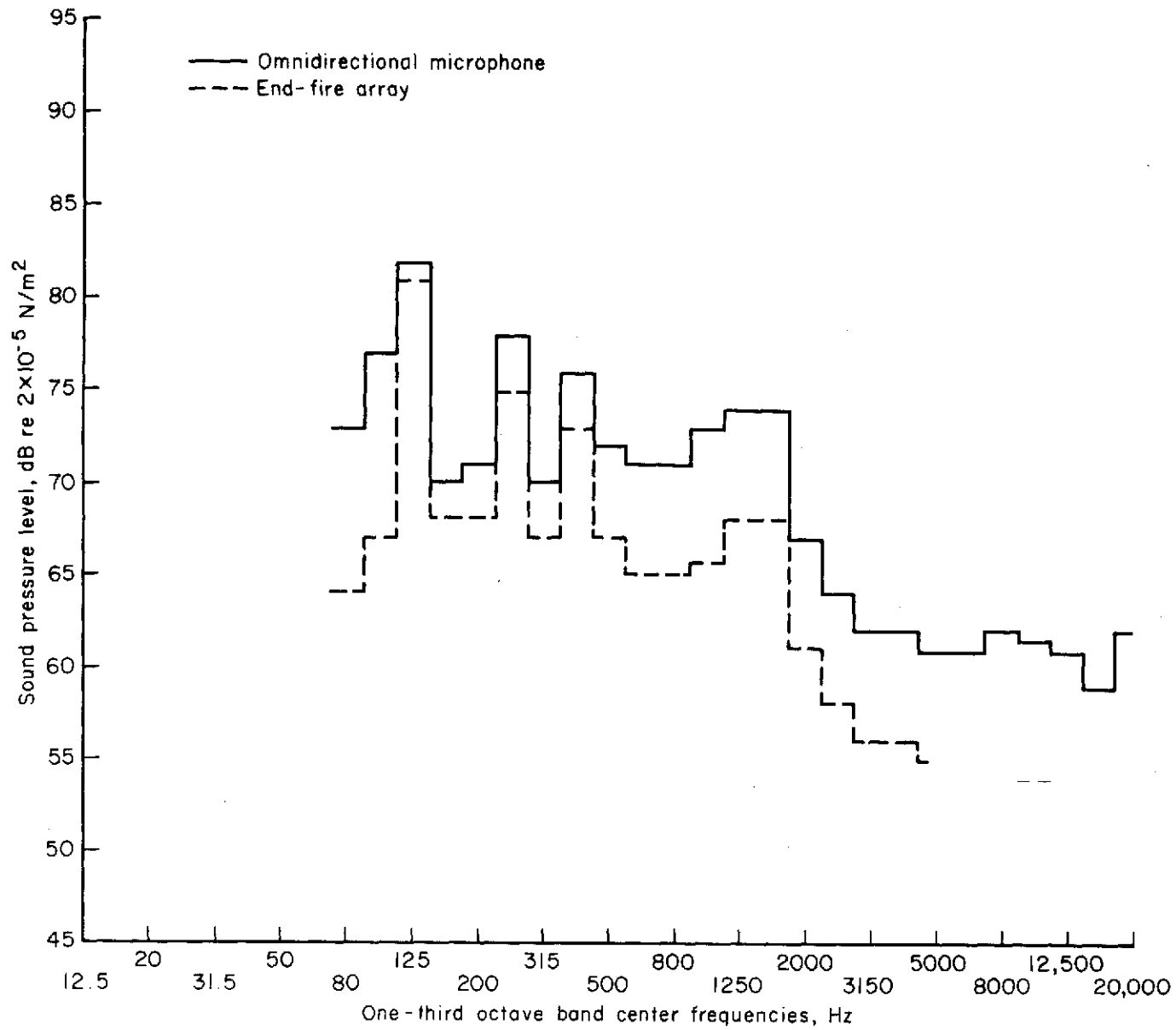
(f) $U = 18 \text{ m/s}$ (58 f/s), 2000 Hz.

Figure 7.— Continued.



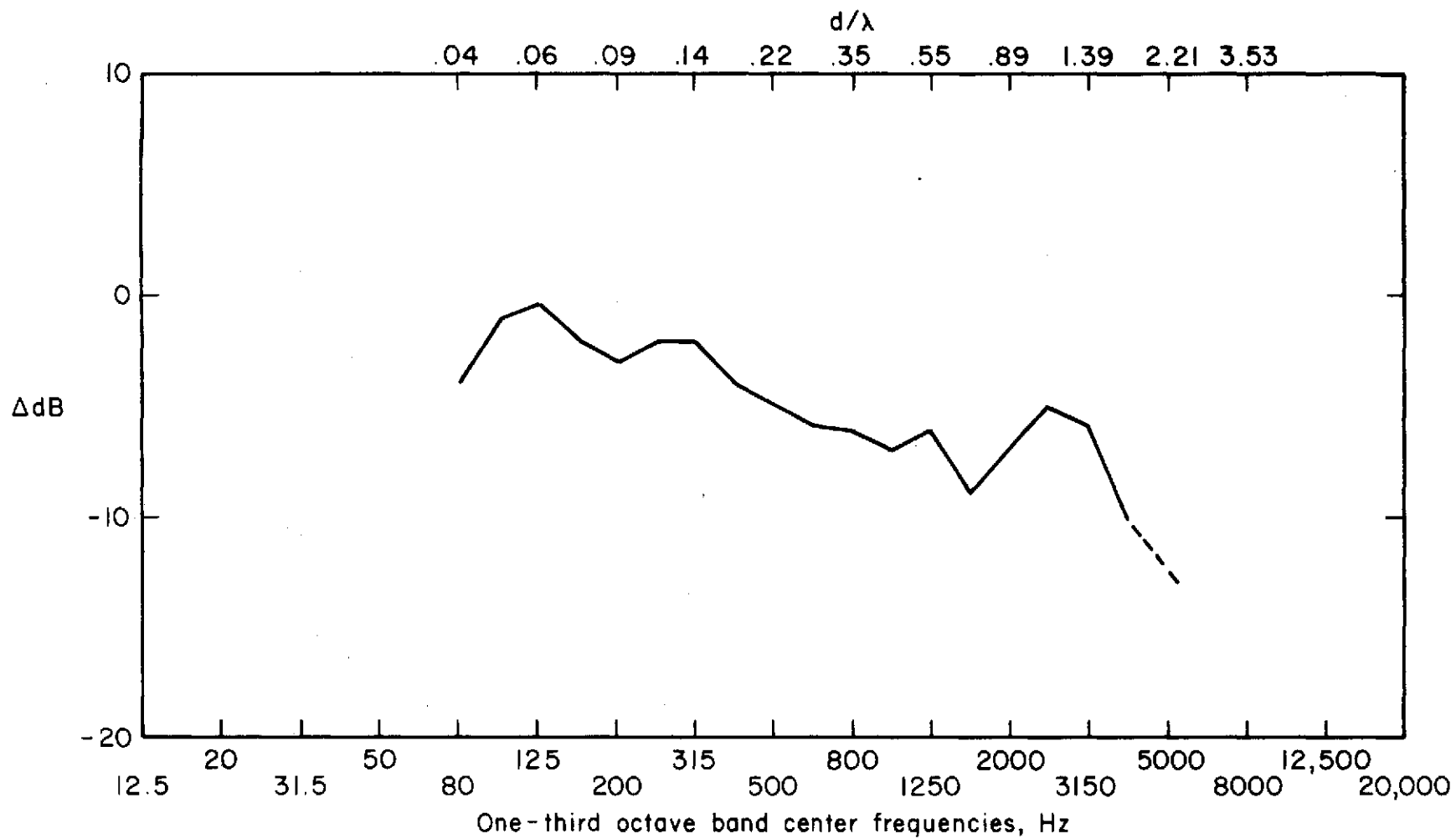
(g) $U = 18$ m/s (58 f/s), 4000 Hz.

Figure 7.— Continued.



(h) $U = 28$ m/s (92 f/s), 1000 Hz.

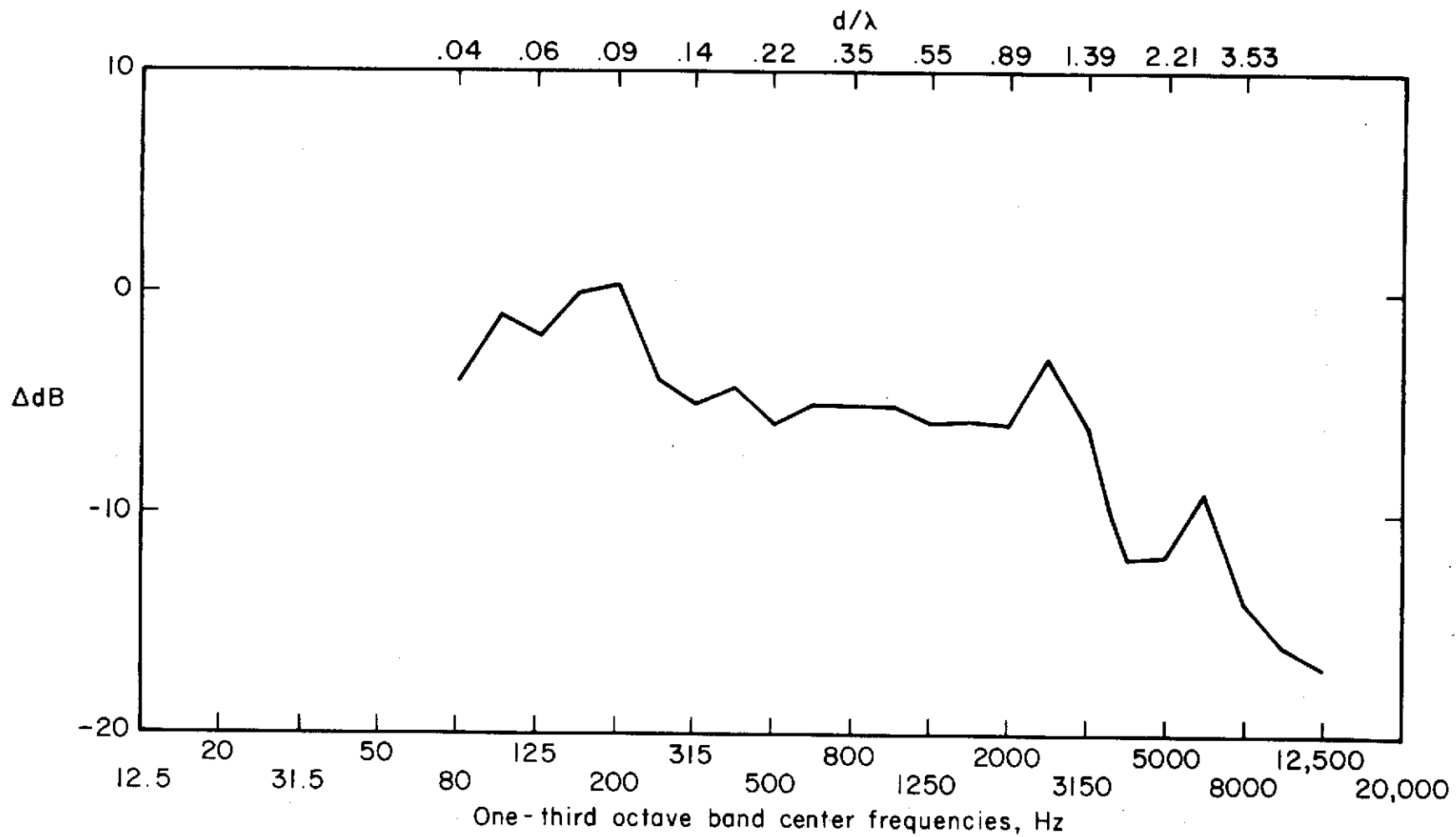
Figure 7.— Concluded.



(a) Horn off, $U = 18 \text{ m/s}$ (58 f/s).

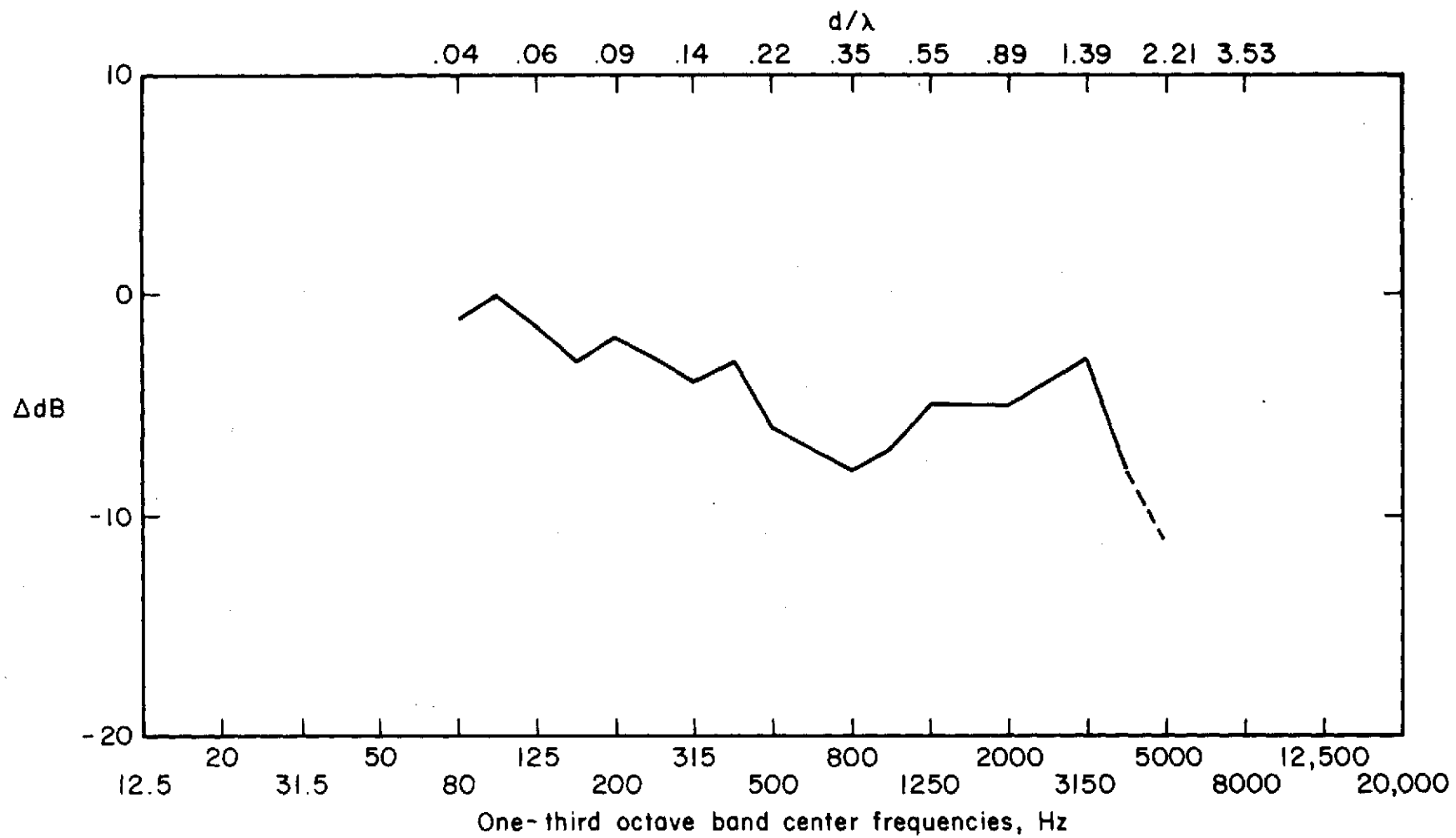
Figure 8.— Reduction of reverberant and background noise by the array,

$$\Delta dB = dB_{\text{array}} - dB_{\text{omnidir. mic.}}$$



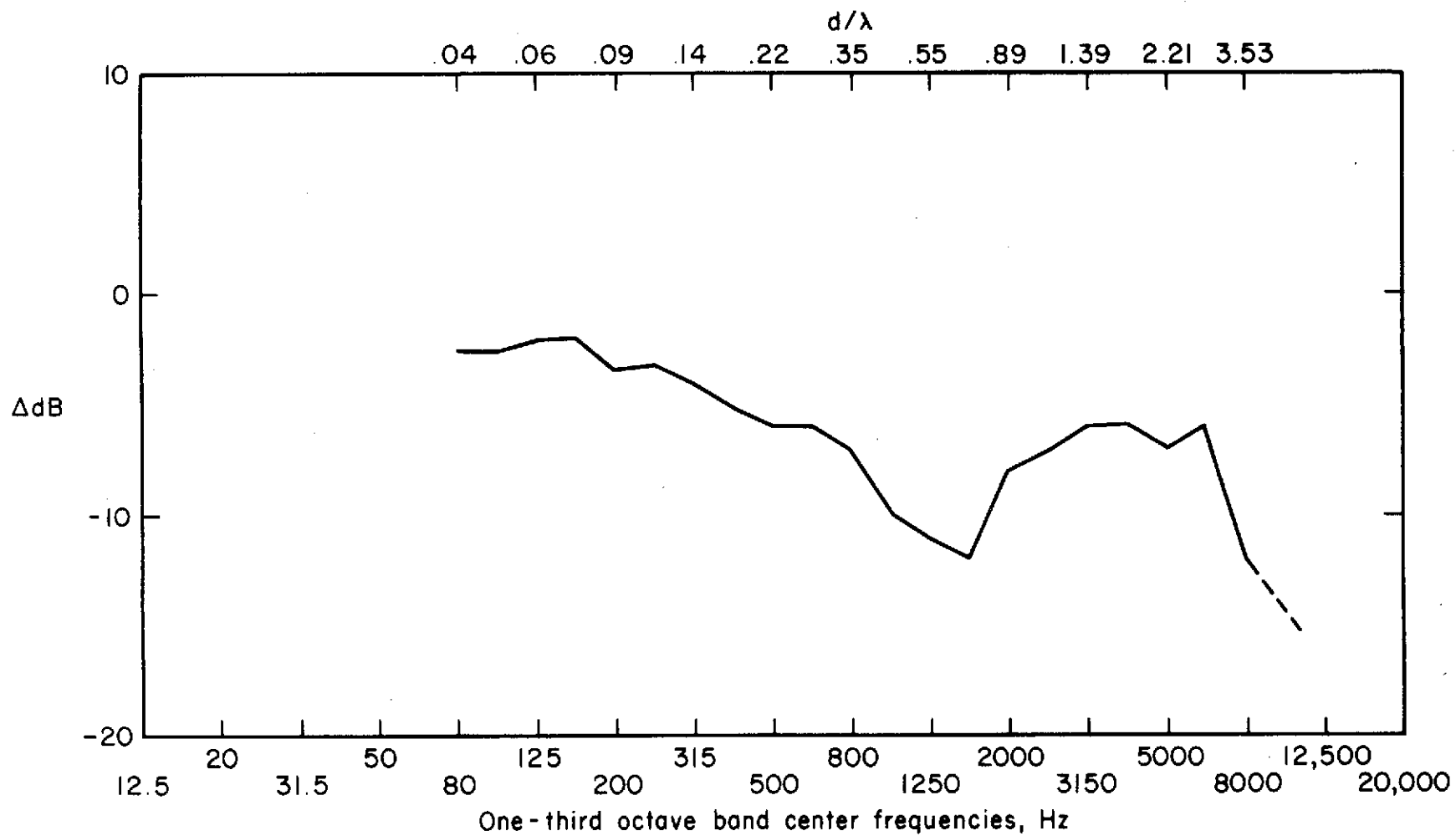
(b) $U = 0$, 1000 Hz source.

Figure 8.— Continued.



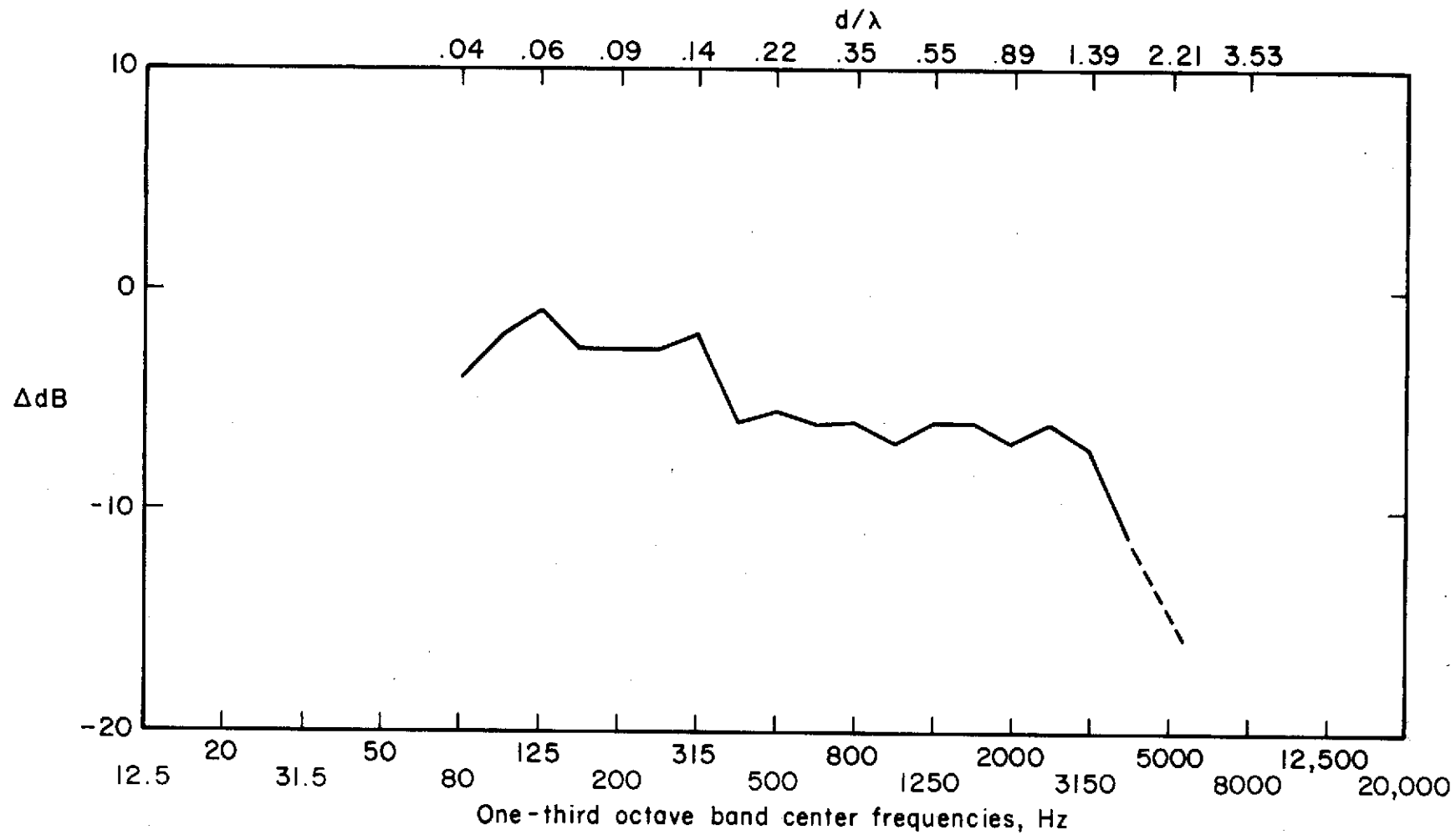
(c) $U = 0$, 2000 Hz.

Figure 8.— Continued.



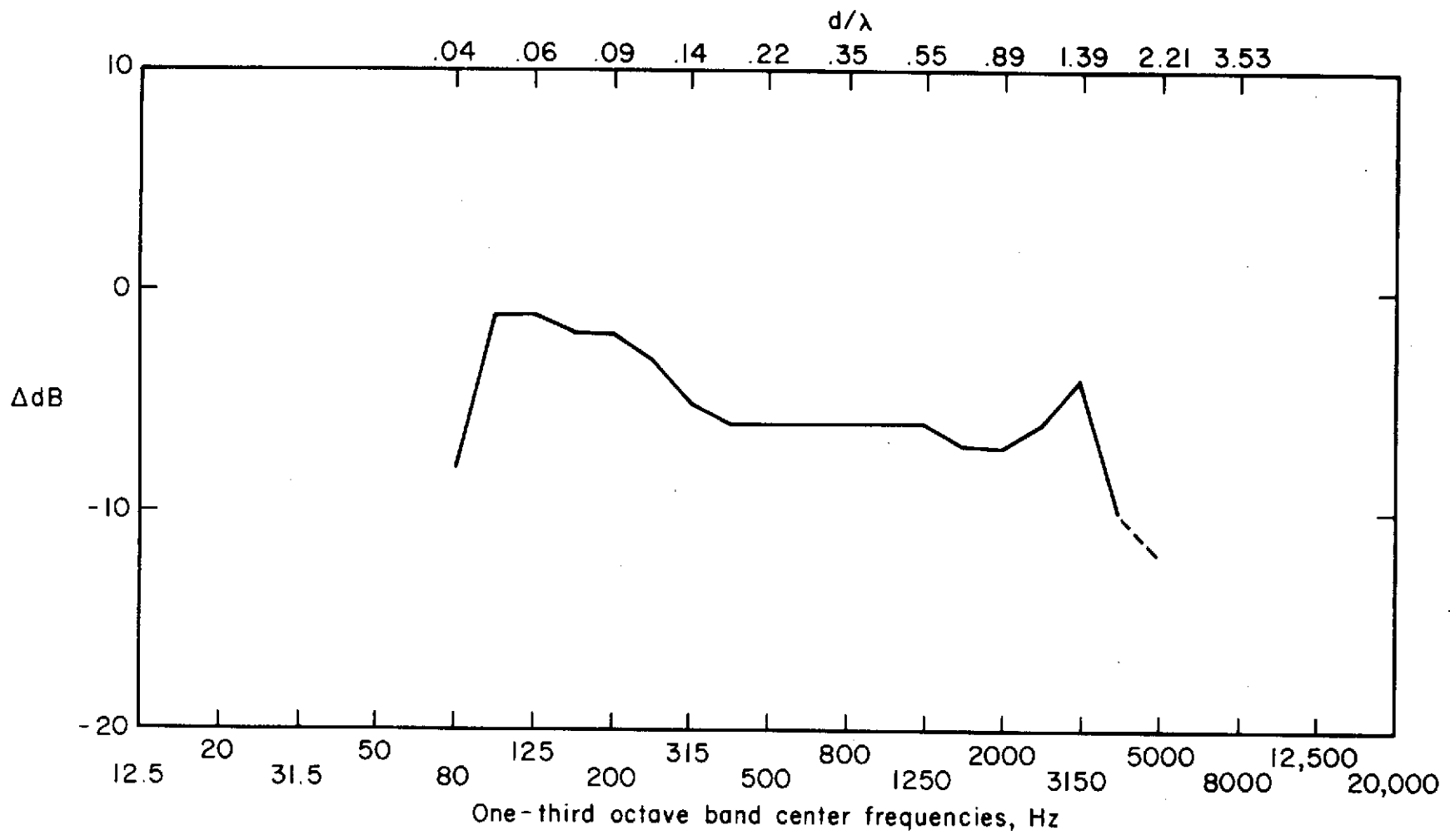
(d) $U = 0$, 4000 Hz.

Figure 8.— Continued.



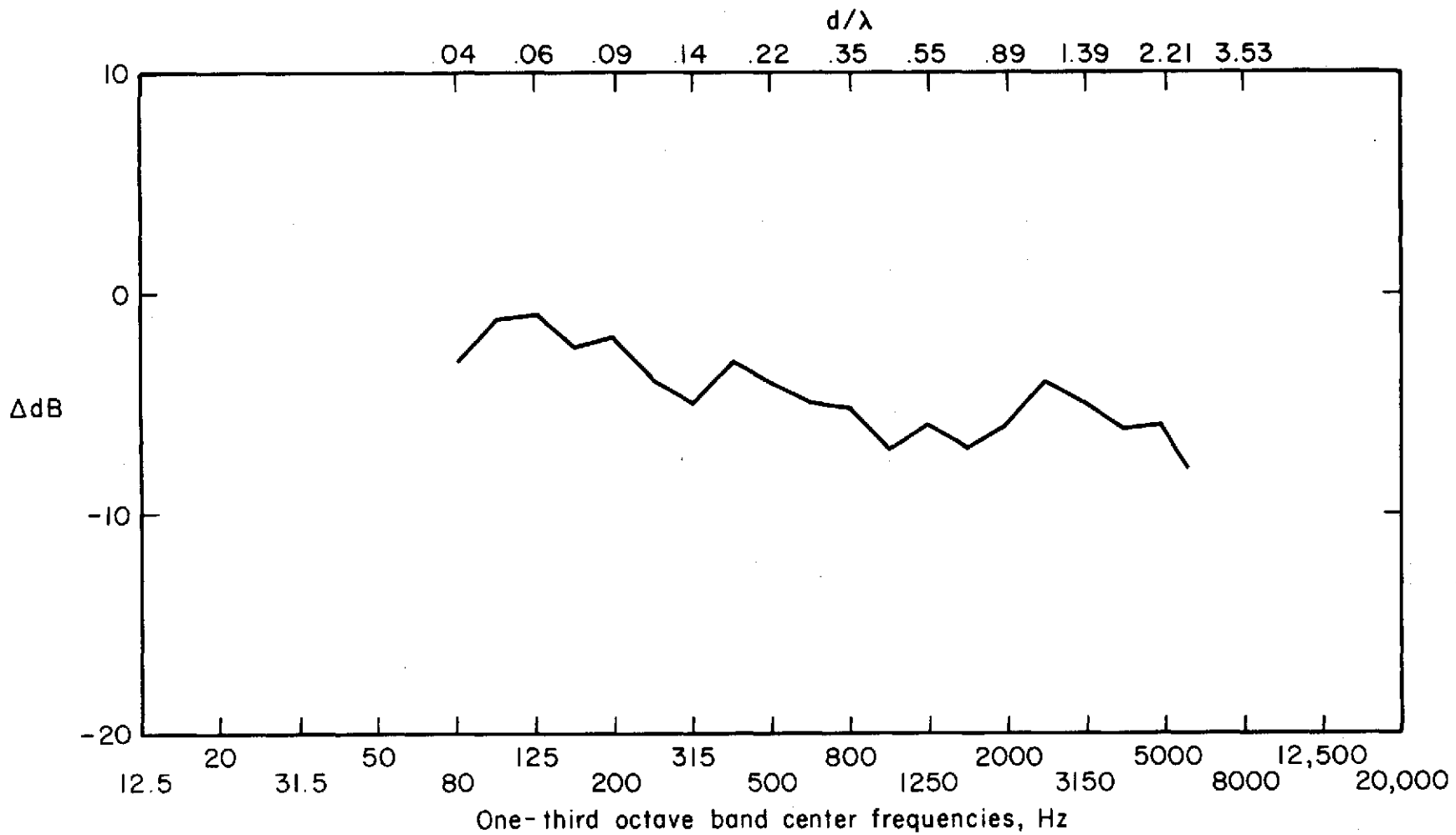
(e) $U = 18 \text{ m/s}$ (58 f/s), 1000 Hz.

Figure 8.— Continued.



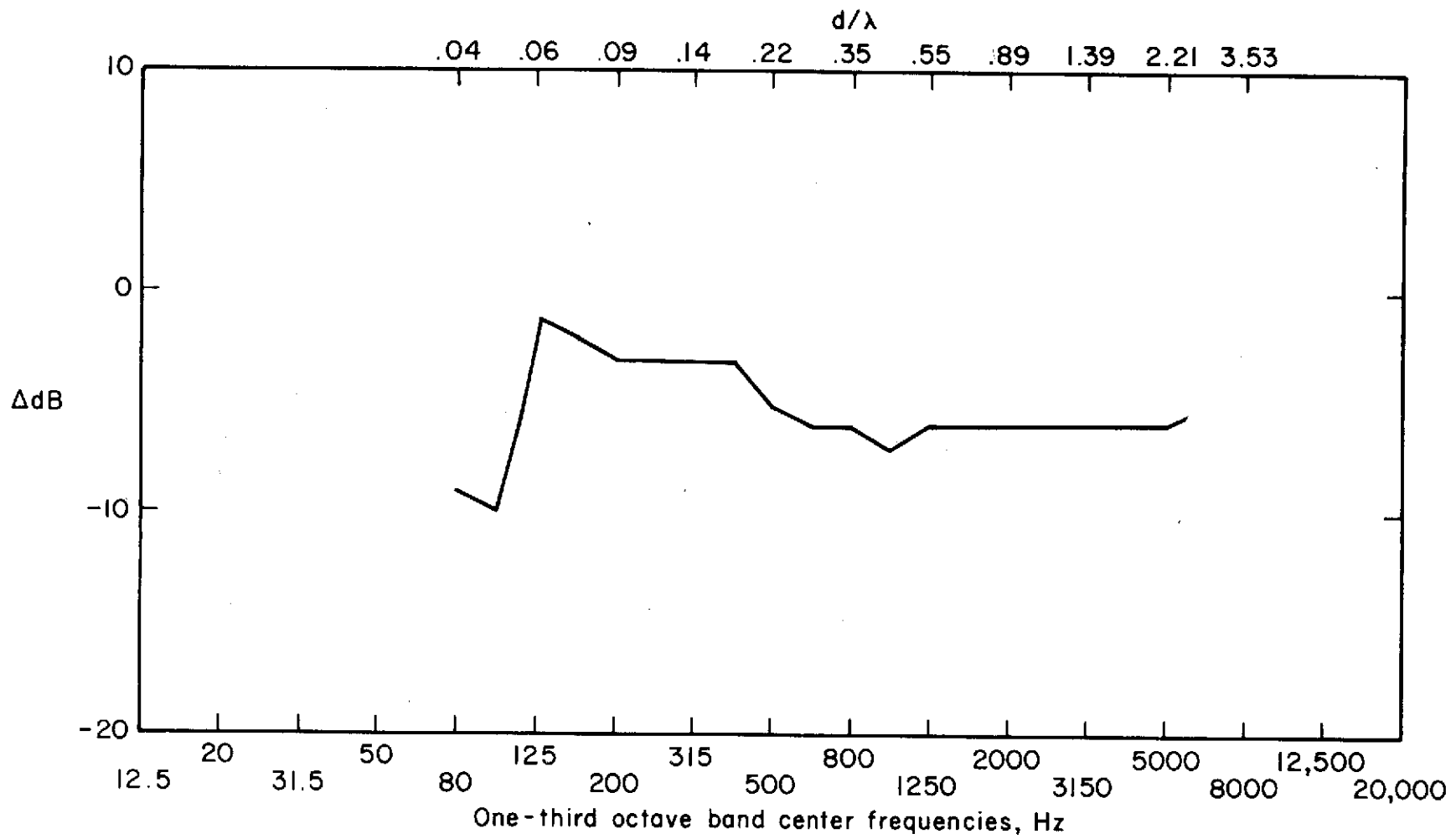
(f) U = 18 m/s (58 f/s), 2000 Hz.

Figure 8.— Continued.



(g) $U = 18 \text{ m/s}$ (58 f/s), 4000 Hz.

Figure 8.— Continued.



(h) $U = 28 \text{ m/s}$ (92 f/s), 1000 Hz .

Figure 8.— Concluded.

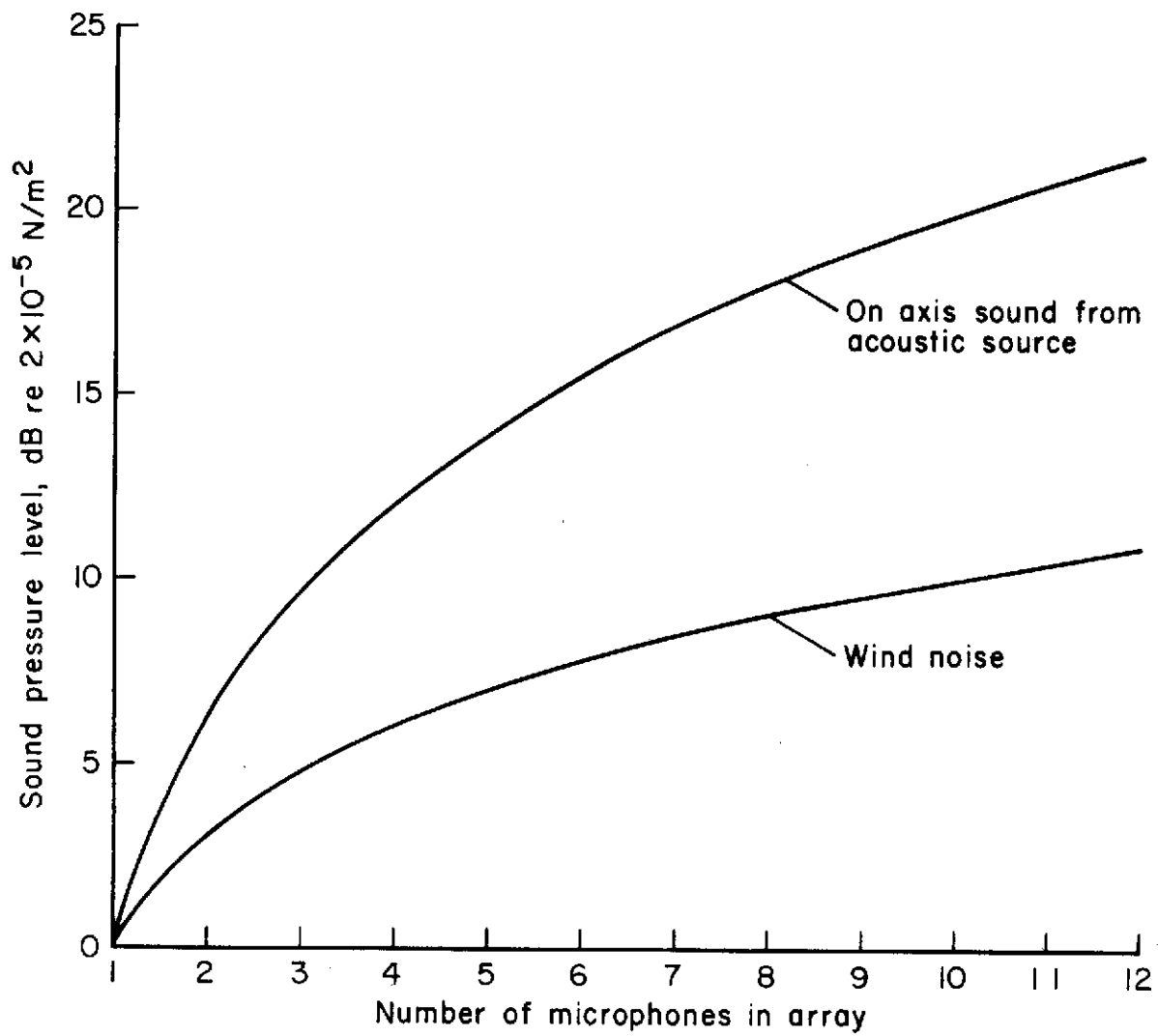


Figure 9.— Predicted array output in excess of single microphone output.

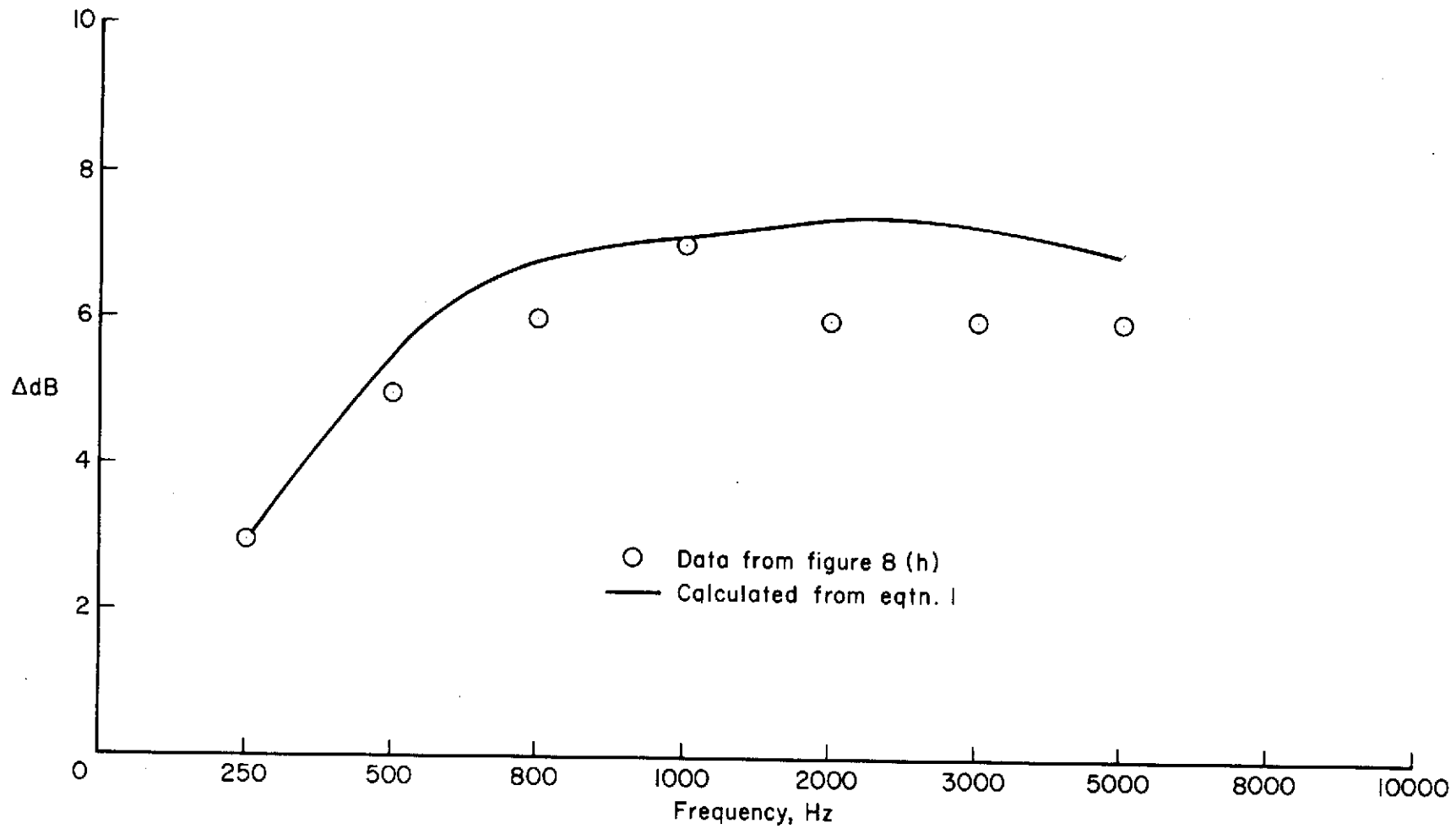


Figure 10.— Calculated and measured noise rejection of array;
 Δ dB = dB_{omnidir. mic.} - dB_{array}